Universidade de Aveiro Departamento de Biologia
2015

Telma Filipa da Silva Martins

Role of the sphingomyelinase Isc1p in the regulation of iron homeostasis in *Saccharomyces cerevisiae*

O papel da esfingomielinase Isc1p na regulação da homeostasia do ferro em *Saccharomyces cerevisiae*

DECLARAÇÃO

Declaro que este relatório é integralmente da minha autoria, estando devidamente referenciadas as fontes e obras consultadas, bem como identificadas de modo claro as citações dessas obras. Não contém, por isso, qualquer tipo de plágio quer de textos publicados, qualquer que seja o meio dessa publicação, incluindo meios eletrónicos, quer de trabalhos académicos

Universidade de Aveiro Departamento de Biologia
2015

Telma Filipa da Silva Martins

Role of the sphingomyelinase Isc1p in the regulation of iron homeostasis in *Saccharomyces cerevisiae*

O papel da esfingomielinase Isc1p na regulação da homeostasia do ferro em *Saccharomyces cerevisiae*

Dissertação apresentada à Universidade de Aveiro para cumprimento dos requisitos necessários à obtenção do grau de Mestre em Biologia Molecular e Celular, realizada sob a orientação científica da Doutora Clara Isabel Ferreira Pereira, Investigadora de Pós-doutoramento no Instituto de Biologia Molecular e Celular do Porto, Professora Doutora Anabela Pinto Rolo, Professora Auxiliar do Departamento de Ciências da Vida da Universidade de Coimbra e Professora Doutora Maria de Lourdes Gomes Pereira, Professora Associada com Agregação do Departamento de Biologia da Universidade de Aveiro.

This work was funded by FEDER (Fundo Europeu de Desenvolvimento Regional) through the program "Programa Operacional Fatores de Competitividade – COMPETE and by FCT (Fundação para a Ciência e a Tecnologia) through the project FCOMP-01-0124-FEDER-028210 (PTDC/BBB-BQB/1850/2012).

Aos meus Pais e ao Mário,

“O começo de todas as ciências é o espanto de as coisas serem o que são”
Aristóteles

o júri

presidente	Prof.ª Doutora Helena Silva professora auxiliar do Departamento de Biologia da Universidade de Aveiro
orientadora	Doutora Clara Isabel Ferreira Pereira investigadora no grupo de investigação de Sinalização Celular Redox no Instituto de Biologia Molecular e Celular do Porto
arguente	Doutora Isabel João Soares da Silva investigadora no grupo de investigação de Nefrologia e Doenças Infeciosas no Instituto Nacional de Engenharia Biomédica

agradecimentos

Antes de mais quero agradecer à minha orientadora Dra. Clara Pereira, pela excelente orientação, apoio, motivação, disponibilidade, confiança, pelos conselhos e ensinamentos transmitidos, e também pela sua amizade. Obrigada pelo constante acompanhamento durante este período.
Quero também agradecer ao Prof. Vítor Costa, por me ter acolhido e ter possibilitado a realização da minha tese de Mestrado no seu grupo de investigação, por todo o apoio e pelos conhecimentos partilhados. Obrigada pelo voto de confiança.
Agradeço a todos os elementos dos grupos RCS, MCA e MicroBiosyn que me receberam da melhor forma desde o primeiro dia. Em especial, a todos os colegas de laboratório pelos ensinamentos, pela amizade e por estarem sempre disponíveis para me ajudarem, ao Ivo, ao Vítor, à Vanda, à Rita, ao Nuno, à Rute, à Sílvia e ao Filipe.
Quero agradecer ao Dr. Jery Kaplan e ao Dr. Yamaguchi Iwai Yuko pelo fornecimento dos plasmídeos pRS426-*GFP-AFT1*, pRS416-*AFT1-SD-HA* e pRS416-*AFT1-HA*.
À Dra. Andreia Leite e à Dra. Maria Rangel por generosamente fornecerem a sonda AL1. E, por fim, quero agradecer ao Dr. Vítor Teixeira pela extracção dos vaúolos, que me permitiu analisar o ferro e por estabelecer o contacto com a Dra. Andreia Leite e a Dra. Maria Rangel.
Aos meus amigos e a todos os meus colegas, pela amizade e pelo companheirismo nesta etapa do meu percurso. Um especial agradecimento à Carina, pelo apoio nos dias menos bons e pela sua disponibilidade para me ajudar sempre que preciso.
Ao Mário, por ter estado sempre ao meu lado, por todo o amor, amizade, confiança, carinho, por respeitar sempre as minhas decisões, compreensão e apoio que ao longo destes anos me deram força para ultrapassar os momentos menos bons.
À minha família pelo apoio incondicional, e mais importante, um especial agradecimento aos meus Pais, por todo o apoio, amor, compreensão, carinho e motivação, e pelo esforço que fizeram para que tudo fosse possível.

A todos, um sincero Obrigada.

palavras-chave Isc1p, Esfingolípidos, Ferro, Ferro ferroso, Ferro férrico, Aft1p e *Stress* oxidativo.

resumo

O Ferro é um elemento essencial para a viabilidade celular, sendo um componente de diversas metaloproteínas, contendo grupos de ferro e enxofre e centros heme. A capacidade de ganhar e perder eletrões, alterando entre os estados ferroso (Fe^{2+}) e férrico (Fe^{3+}), faz com que o ferro esteja envolvido em diversos processos celulares. Os sistemas de aquisição de ferro têm de ser altamente regulados para assegurar um fornecimento contínuo de ferro e simultaneamente prevenir a sua toxicidade associada à formação de radicais hidroxilo pela reação de Fenton. A perda da homeostasia do ferro está associada a muitas patologias, o que enfatiza a importância do estudo dos mecanismos envolvidos na homeostasia do ferro.

A proteína inositolfosfoesfingolípido fosfolipase C (Isc1p) presente em *Saccharomyces cerevisiae* hidrolisa esfingolípidos complexos para produzir ceramida, um esfingolípido bioativo. A deleção do *ISC1* é caracterizada pelo envelhecimento celular prematuro, sensibilidade ao stresse oxidativo e disfunção mitocondrial. Este mutante também exibe uma sobreexpressão dos genes envolvidos na captação de ferro, resultando em níveis elevados de ferro. No entanto, a fase do crescimento em que a acumulação do ferro ocorre, o compartimento específico de acumulação ou mesmo o estado de oxidação do ferro acumulado nas células *isc1*Δ permanece por caracterizar. Além disso, os mecanismos moleculares subjacentes à acumulação de ferro nas células *isc1*Δ não são conhecidos.

Monitorizando os níveis de ferro e o estado de oxidação ao longo do crescimento, foi possível observar que a deleção do *ISC1* causou uma acumulação de ferro em todas as fases de crescimento em ambas as formas ferrosa e férrica. Além dos níveis de ferro elevados, as células *isc1*Δ também exibiram uma alteração na distribuição de ferro no interior da célula. Ao contrário das células wt, as células *isc1*Δ não acumularam ferro férrico no vacúolo, mas em vez disso, o ferro pareceu estar distribuído por toda a célula. Adicionalmente, a acumulação de ferro nas células *isc1*Δ foi associada à ativação do Aft1p, o ativador transcricional sensível a níveis baixos de ferro. Células sem a proteína Isc1p exibiram níveis mais elevados de Aft1p retido no núcleo e a delecção do *AFT1* suprimiu a acumulação de ferro observada no mutante *isc1*Δ. Também se observou que a defosforilação do Aft1p nas células *isc1*Δ está associada à sua ativação.

Adicionalmente, a ativação da fosfatase Sit4p nas células *isc1*Δ como um potencial mecanismo responsável pela defosforilação e ativação do Aft1p foi descartada, uma vez que as células *isc1*Δ*sit4*Δ continuam a apresentar acumulação de ferro.

Em conclusão, estes resultados indicam que a defosforilação e ativação do Aft1p é o fator responsável pela acumulação de ferro no mutante *isc1*Δ e reforça o papel do Isc1p na regulação da homeostasia do ferro.

keywords Isc1p, Sphingolipids, Iron, Ferrous iron, Ferric iron, Aft1p and oxidative stress.

abstract

Iron is an essential element for cell viability since it is a component of several metalloproteins, containing iron-sulfur clusters and heme centers. The ability to gain and lose electrons, switching between the ferrous (Fe^{2+}) and ferric (Fe^{3+}) states, renders the involvement of iron in many cellular processes. Iron acquisition systems have to be highly regulated to assure a continuous supply of iron but simultaneously prevent its toxicity associated with the formation of hydroxyl radicals by the Fenton reaction. Loss of iron homeostasis is behind many pathologies, highlighting the importance of understanding the mechanisms involved in iron homeostasis.

The *Saccharomyces cerevisiae* inositolphosphosphingolipid phospholipase C (Isc1p) hydrolyses complex sphingolipids to produce ceramide, a bioactive sphingolipid. *ISC1* deletion is characterized by premature aging, oxidative stress sensitivity and mitochondrial dysfunction. This mutant also exhibits an up regulation of genes involved in iron uptake leading to increased levels of iron. However the growth phase in which iron accumulation occurs, the specific site of accumulation or even the oxidation state of the accumulated iron in *isc1*Δ cells remains uncharacterized. Futhermore, the molecular mechanisms behind the iron overload in *isc1*Δ cells are not known.

By monitoring iron levels and oxidation state along growth, it was possible to observe that deletion of *ISC1* caused iron accumulation in all phases of growth in both the ferric and ferrous forms. Additionally to the increased iron levels, *isc1*Δ cells also exhibited an altered distribution of iron within the cell. Unlike wild type, *isc1*Δ cells did not accumulate ferric iron in the vacuole, but instead, iron seemed to be distributed throughout the cell. Furthermore, iron accumulation in *isc1*Δ cells was associated with the activation of Aft1p, the low iron-sensing transcriptional activator. Cells lacking Isc1p exhibed higher levels of Aft1p retained in the nucleus, and *AFT1* deletion abolished iron accumulation in the *isc1*Δ mutant. It was also found that dephosphorylation of Aft1p in *isc1*Δ cells is associated with its activation. Additionally the activation of the phosphatase Sit4p in *isc1*Δ cells was discarded as a potential mechanism behind Aft1p dephosphorylation and activation, since *isc1*Δ*sit4*Δ cells still exhibit iron overload.

Overall, these results indicate that the dephosphorylation and activation of Aft1p is the factor behind the accumulation of iron in the *isc1*Δ mutant and reinforce the role of Isc1p in the regulation of iron homeostasis.

TABLE OF CONTENTS

TABLE LIST

FIGURE LIST

GENERAL ABREVIATIONS

BCA	Bicinchoninic acid
BPS	Bathophenanthroline disulfonic acid
Cer	Ceramide
CFUs	Colony-forming units
CL	Cardiolipin
CLS	Chronological lifespan
COX	Cytochrome *c* oxidase
DAPI	4'-6-Diamidino-2-phenylindole
dhCer	Dihydroceramide
dhSph	Dihydrosphingosine or Sphinganine
DNA	Deoxyribonucleic acid
dNTPs	Deoxynucleotides
EDTA	Ethylenediamine tetraacetic acid
Fe/S	Iron sulfur
HOG pathway	Osmotic glycerol pathway
IPC	Inositolphosphoceramide
LB	Lysogeny broth
LCB	Long-chain base
MAPK	Mitogen-activated protein kinase
MIPC	Mannosylinositol phosphorylceramide
$M(IP)_2C$	Mannose diinositolphosphoceramide
PBS	Phosphate buffered saline
PCR	Polymerase chain reaction
pDNA	Plasmid DNA
PDS	Post-diauxic-shift
PEG	Polyethylene Glycol
PG	Phosphatidylglycerol
PhytoCer	Phytoceramide
PhytoSph	Phytosphingosine

PS	Phosphatidylserine
$R^{\cdot}$	Thiyl radicals
$RO^{\cdot}$	Alkoxyl radicals
$ROO^{\cdot}$	Peroxyl radicals
ROS	Reactive oxygen species
$RSOO^{\cdot}$	Thiyl-peroxyl radicals
SC	Synthetic complete
SDS	Sodium dodecyl sulfate
Sph	Sphingosine
TAE	Tris-acetate-EDTA
TBS	Tris-buffered saline
Tris	Tris (hydroxymethyl) aminomethane
Tris-HCL	Tris-Hydrocloride
TTBS	Tris-buffered saline plus Tween
wt	Wild type
YPD	Yeast peptone dextrose

1. INTRODUCTION

1.1. Iron homeostasis in *Saccharomyces cerevisiae*

1.1.1. Iron – general concepts

Iron is an essential element required for survival of almost all organisms. Major cellular components, such as proteins, nucleic acids, and lipids (unsaturated fatty acids, sterol and sphingolipids) require iron for its biosynthesis. In metalloproteins, iron can be found as prosthetic group in various forms: elemental iron, oxoiron or oxorion-zinc, heme, and iron-sulfur (Fe/S) clusters. Due to its huge ability to gain and lose electrons, switching between the ferrous (Fe^{2+}) and ferric (Fe^{3+}) states, iron is involved in many cellular processes such as electron transfer (e.g., in the mitochondrial respiratory chain), oxygen sensing by hydroxylases, catalysis in many enzymatic reactions (e.g., in the tricarboxylic acid cycle), DNA replication and repair [1–4].

The same property that makes iron an indispensable nutrient also makes it extremely toxic, because under aerobic conditions, iron can catalyse the generation of reactive oxygen species (ROS) through the Fenton Reaction. Iron may generate hydroxyl radicals ($HO^{\cdot}$) when Fe^{2+} reacts with hydrogen peroxide (H_2O_2) and superoxide anions ($O_2^{\bullet-}$) through the reaction between Fe^{2+} with oxygen. Heme iron (either free or within hemoproteins) can also catalyse the formation of radicals, mainly via formation of oxoferryl intermediates. Finally, iron can also catalyze the generation of organic reactive species, such as peroxyl ($ROO^{\cdot}$), alkoxyl ($RO^{\cdot}$), thiyl ($RS^{\cdot}$), or thiyl-peroxyl ($RSOO^{\cdot}$) radicals [4,5]. These highly reactive species promote the oxidation of proteins, peroxidation of membrane lipids, and modification of nucleic acids. ROS are inevitable cellular byproducts and cells have enzymatic systems capable of either preventing or removing oxygen radicals once formed. An excess of steady state levels of ROS beyond the antioxidant capacity of the organism is called oxidative stress. Oxidative stress is commonly found in several pathological conditions [6]. Increased levels of redox reactive iron aggravates oxidative stress and leads to accelerated cellular damage [4]. This situation is illustrated in diseases of iron overload, such as hereditary hemochromatosis, where excessive iron accumulation results in tissue damage and organ failure [7]. In organisms that do not have regulated mechanism to extrude iron (e.g., yeast), the regulation of iron uptake is one of the most critical steps in maintaining iron homeostasis [2].

1.1.2. Ion uptake

Although iron is the second most abundant metal in the crust of the earth, its bioavailability is low, because under aerobic conditions, it is predominantly present as $Fe^{3+,}$ which is poorly soluble to the cells at physiological pH. Therefore, organisms developed several strategies to uptake iron. Many bacteria, plants and some fungi synthesize molecules called siderophores that are able of chelating iron by binding to Fe^{3+} and allowing its transport into the cell. Although *Saccharomyces cerevisiae* do not produce their own siderophores, it can capture siderophores produced by other organisms [2,4,8].

Fungal siderophore iron uptake is mediated by plasma membrane permeases, all of which are members of the major facilitator superfamily [9,10]. *S. cerevisiae* produces at least four distinct facilitators for their uptake: Arn1p (facilitator specific for a class of ferrichromes) [11], Arn2p/Taf1p (facilitator specific for triacetylfusarinine) [12], Arn3p/Sit1p (ferrioxamine B facilitator) [13], and Arn4p/Enb1p (facilitator specific for ferric enterobactin) [14]. Retention of iron-siderophore chelates in the cell wall is facilitated by Fit1p, Fit2p, and Fit3p, three cell wall mannoproteins, involved in enhance iron uptake [15] (Figure 1).

S. cerevisiae also has a reductive iron uptake mechanism in which Fe^{3+} is first reduced to Fe^{2+} state and then Fe^{2+} is transported into cytosol via a Fe^{2+}-specific transport complex. The reduction step is catalysed by members of *FRE* family of metalloreductases (Fre1-4p), heme-containing transmembrane proteins present in the cell surface [16]. In addition to the reduction of Fe^{3+} iron salts, the *FRE* metalloreductases are also involved in the reduction and consequent release of iron from siderophore-iron complexes. Reduced iron can be taken up into cell through a high-affinity or a low-affinity transport complex. High affinity iron transport system, composed of the multicopper oxidase Fet3p [17] and the transmembrane permease Ftr1p [18] transports Fe^{2+} when environmental iron is limiting. In iron-replete environments, Fe^{2+} can be the substrate for the low affinity iron transport system, which is composed of Smf1p [19], an H^{+}/ Fe^{2+} symporter that utilizes the pH gradient to transport iron, and the permease Fet4p [20].

After transport into the cytosol, iron is trafficked to organelles, such as nucleus, endoplasmic reticulum (RE), vacuole and mitochondria. Little is known about the iron content of the cytosol, mainly because of the difficulty of studying cytosolic material. In spite of this, several Fe/S, mononuclear iron proteins, and iron-siderophores molecules have been identified in the cytosol [21].

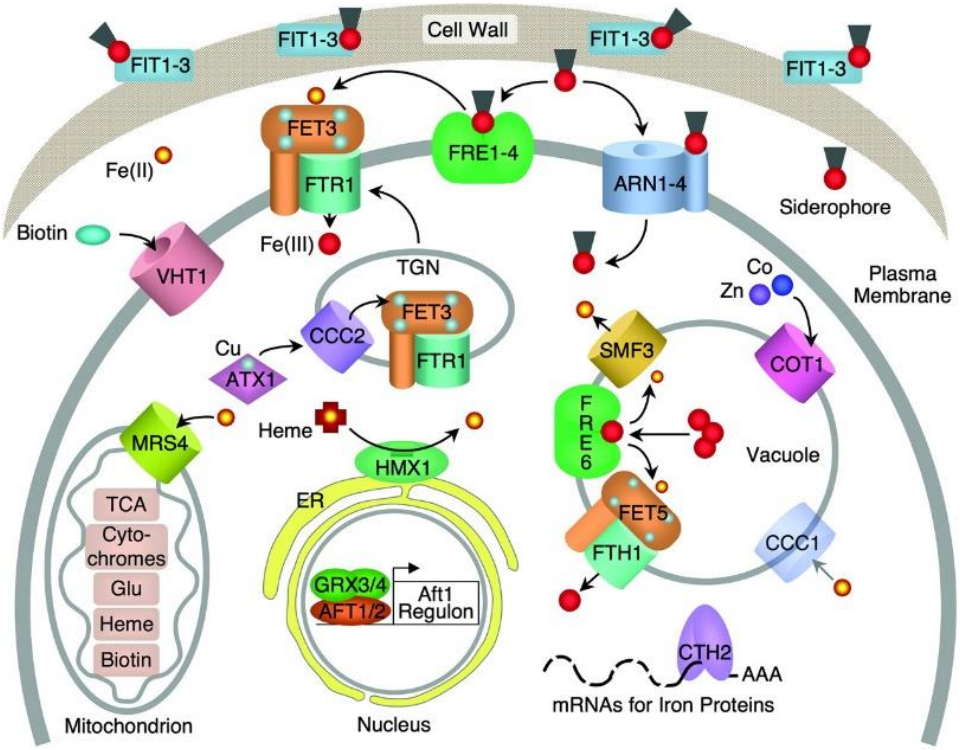

Figure 1 – Schematic illustration of iron uptake and iron mobilization. *S. cerevisiae*, do not produce their own siderophores but still express siderophore transporter genes (ARN1-4), permitting them to capture siderophores produced by other organisms. Retention of iron-siderophore chelates in the cell wall is facilitated by three cell wall mannoproteins (FIT1-3). In addition to siderophore uptake, *S. cerevisiae* can use a reductive iron uptake mechanism. When using this system, Fe^{3+} is reduced to the more soluble Fe^{2+} by cell surface metalloreductases (FRE1-4). The Fe^{2+} generated is the substrate for two distinct iron-transport systems: a low (not represented) and a high affinity (FET3 and FTR1) transport systems.
The mitochondrial transporter MRS4 is involved in the transport of iron into the mitochondria and the vacuolar transporter CCC1 is involved in the transport of iron into the vacuole. Iron can be transported from the vacuole to the cytosol after reduction to Fe^{2+} by one metalloreductases homologous to the plasma membrane (FRE6). FET5 and FTH1, represents the high-affinity transport system and SMF3 the low-affinity transport system, involved in moving iron out of the vacuole [22].

1.1.3. Vacuolar iron storage

Vacuoles are major hubs of iron trafficking and homeostasis in yeast. Vacuoles are the main iron storage compartment, allowing cells to utilize stored iron when extracellular iron is scarce and during the transition from fermenting to respiring metabolism (diauxic

shift). Sequestration of iron within the vacuole also protect cells from the toxic effects of iron, and maintain cellular iron homeostasis, by preventing fluctuation in cytosolic iron [2,23].

When iron is abundant, it is maintained at homeostatic levels by sequestration in the vacuole through the activity of the iron manganese transporter Ccc1p. Iron can also be imported through endocytosis, however the import by Ccc1p is the main pathway responsible for Fe import into vacuoles. The ccc1Δ cells cannot maintain proper iron homeostasis and are more sensitive to high and low extracellular iron concentrations [24]. Ferric siderophores can accumulate as an intact chelate in the cytosol and vacuoles after uptake, indicating that siderophores can also serve as iron storage molecules [22].

Contrariwise, when iron abundance in extracellular media is low, iron is mobilized from the vacuole to the cytosol. Fre6p, one member of the *FRE* family of metalloreductases and homologous to the plasma membrane proteins Fre1-4p, is present on the vacuolar membrane, and is involved in the reduction of vacuolar iron prior to transport into the cytosol [25]. Fet5p and Fth1p, homologues of the plasma membrane high-affinity ferrous iron transport (Fet3p-Ftr1p complex) are involved in the transport of iron across vacuole membrane [26]. Smf3p, a member of the Nramp family of divalent metal transports, represents the low-affinity transport system involved in moving iron out of the vacuole (Figure 1) [27].

Iron in the vacuole consists of Fe^{3+} species. It is not known which exact specie is imported to the vacuole, although it is generally assumed that is Fe^{2+}, and once in the vacuole, it is oxidized to Fe^{3+} probably because the vacuolar lumen is more acidic than the cytosol [23,28]. The acidic environment of the vacuole is required to properly sequester and detoxify iron and to minimize the generation of ROS. Loss of vacuolar H^+-ATPase (V-ATPase) activity, results in the relative vacuolar alkalinisation and cytosolic acidification and this loss of pH homeostasis was shown to result in an iron deficiency signal [29].

1.1.4. Mitochondrial iron metabolism

Mitochondria are also important for iron metabolism and are an important intracellular destination of iron, where it is used for the biosynthesis of heme and Fe/S clusters. Mrs3/4p mediate Fe^{2+} transport across the yeast inner mitochondrial membrane, driven by both the concentration gradient of this ion and pH [30]. Mrs3/4p are high affinity importers of iron that are activated under low iron conditions [31,32]. Rim2p, a member of the

mitochondrial carrier family, was also identified as an iron transporter. Rim2p can substitute Mrs3p and Mrs4p function in *mrs3*Δ*mrs4*Δ cells, and seems to act as a physiological low-affinity iron import system under certain conditions, such as cytosolic iron overload. However, Rim2p does not play a significant role in mitochondrial iron influx under normal physiological conditions, and triple deletion of *RIM2*, *MRS3* and *MRS4* is not lethal, suggesting the existence of other low-affinity mitochondrial iron transporter [33,34]. Recently, Mmt1p and Mmt2p, two homologous members of the cation diffusion facilitator transporter family localized to mitochondria, were identified as mitochondrial iron exporters [35,36].

In mitochondria iron can be found as Fe/S clusters, heme species, and iron nanoparticles. Depending on cellular metabolism and the iron content in the growth medium, the cellular distribution of iron can be different. Respiring cells have less iron associated with vacuoles, and mitochondria contain more iron sulfur clusters and heme species and less non-heme iron species. In fermenting cells, mitochondria have lower levels of respiration-related iron-containing proteins, and more non-heme iron species [37,38].

Cells in iron deficiency conditions must prioritize the use of iron. So, most of the available iron goes to the mitochondria where it is assembled into Fe/S clusters and heme centers, prosthetic groups that are critical for cellular metabolism. Little iron is stored in vacuoles and little is present as Fe^{3+} nanoparticles. In cells grown in media with sufficient iron the mitochondria remains the site where much imported iron is sent for Fe/S cluster and heme synthesis and additional iron is present in the vacuoles as Fe^{3+} species [39].

1.1.5. Low iron-sensing transcriptional activator Aft1p/Aft2p

As refereed above, the regulation of iron uptake is one of the most critical steps for maintaining cellular iron homeostasis. At the transcriptional level iron uptake is regulated by the major transcription factor Aft1p, and its paralogue Aft2p [40–42]. In response to iron deficiency, these transcription factors are involved in the activation of the iron regulon, which includes proteins required for iron transport at the plasma membrane, vacuolar iron transport, and mitochondrial iron metabolism, resulting in the mobilization of iron from extracellular sources and intracellular stores. Aft1p and Aft2p have overlapping and separate DNA targets. Aft1p specifically activates the transcription of genes involved in cell surface

iron uptake systems, while Aft2p specifically activates the transcription of genes involved in vacuolar and mitochondrial iron sub-compartmentation and use [43–45].

In addition to iron uptake, Aft1p also activates the expression of Cth1p and Cth2p, paralogous mRNA-binding proteins that facilitate the decay of mRNAs encoding proteins that function in iron-rich metabolic pathways, such as respiration, the tricarboxylic acid cycle, heme biosynthesis, amino acid, sterol, fatty acid metabolism, and mitochondrial Fe/S cluster biogenesis [45–47]. During prolonged iron deficiency, Cth2p also downregulates vacuolar iron storage via CCC1 mRNA degradation to allow adaptation to extended iron depletion [48].

Aft1p localization is important for this regulation. Aft1p is localized in the nucleus in low iron conditions, where it activates the transcription of its target genes, and is translocated to the cytoplasm when there is excess iron (Figure 2) [49].

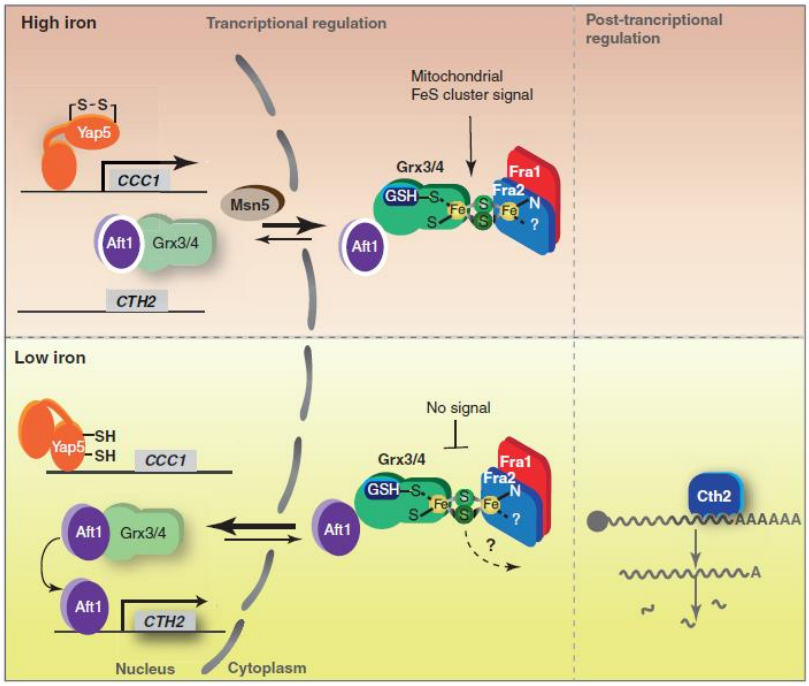

Figure 2 – Schematic illustration of nucleocytoplasmic localization of Aft1p during high and low iron conditions. At high iron conditions, due to interaction to Grx3/4p, Aft1is exported to the cytosol and their export is mediated by Msn5p. On the other hand, under low iron conditions, Aft1 is located in the nucleus, where it activates transcription of the iron regulon [50].

Nucleocytoplasmic localization of Aft1p is regulated by the importin Pse1p [51] and the exportin Msn5p [52]. Although Pse1p-mediated nuclear import of Aft1p is not affected by the iron status of cells, the export of Aft1p by Msn5p occurs in iron-dependent manner. Two regions of Aft1p (aminoacids 147-270 and 301-498) were identified as necessary for Aft1p-Msn5p interaction, as well as for nuclear export of Aft1p in iron replete conditions [52]. Phosphorylation of S210 and S224 (region 147-270) is crucial for Aft1p-Msn5p interaction and phosphorylation of T421, T423, T431, and T435 (region 301-498) is also involved in Aft1p-Msn5p interaction, although it is dispensable. The construction of a phosphoresistent mutant (Aft1p-SA) and a phosphomimetic mutant (Aft1p-SD), in which serine residues S210 and S224 were replaced with alanines or phosphomimetic aspartates, respectively, allowed to ascertain that phosphorylation of S210 and S224 is essential to Msn5p-mediated nuclear export of Aft1p in iron replete conditions, since Aft1p-SA is localized in the nucleus even in the presence of excess iron. However, phosphorylation of S210 and S224 is not the only signal required for iron-dependent nuclear export of Aft1p, because in conditions of iron depletion, Aft1p-SD is still retained in the nucleus. Therefore S210 and S224 phosphorylation is not enough to create a signal for iron-dependent nuclear export of Aft1p in physiological low iron conditions, but additional regulatory mechanism must exist to cope with extreme iron depletion.

Intermolecular interaction of Aft1p also seems to be critical for the recognition of Aft1p by Msn5p. The residue Cys291 of Aft1p is critical for this interaction in the presence of iron since it is disrupted when Cys291 is mutated to phenylanine and consequently Aft1p fails to interact with Msn5p [52].

Although the interaction with Msn5p is important for Aft1p nuclear export under iron-replete conditions, it is not essential for the inhibition of its transcriptional activity, since Aft1p activity is inhibited in *msn5*Δ cells under iron-replete conditions, despite constitutive nuclear localization. Instead, dissociation of Aft1p from its target DNA is the critical step in the regulation of iron metabolism by Aft1p [53]. This dissociation requires the extramitochondrial monothiol glutaredoxins Grx3p and Grx4p. It was observed that association between Grx3/4p and Aft1p is required for dissociation of Aft1p from its target promoters in response to iron repletion and that the Aft1p residues Leu99, Leu102, Cys291, and Cys293 are involved in this interaction. It was also observed that dimerization of Grx3/4p is necessary for Aft1p-Grx3/4p interaction and iron binding to Grx3/4p is required

to its dimerization. Furthermore, Atm1p, the mitochondrial ABC transporter, which has been suggested to be an exporter of Fe/S clusters, is important to both binding of Grx3p to iron and binding of Grx3p to Aft1p under iron replete conditions. This suggests that Fe/S clusters may be the signal for cellular iron content (Figure 3). Other studies have also suggested that Fe/S clusters are involved in Aft1p regulation. Defects in proteins at the mitochondrial Fe/S cluster machinery result in constitutive expression of Aft1p-regulated genes [54,55]. Atm1p is also involved in the export of heme, however it has been demonstrated that heme is not required for Aft1p inhibition by iron [56,57].

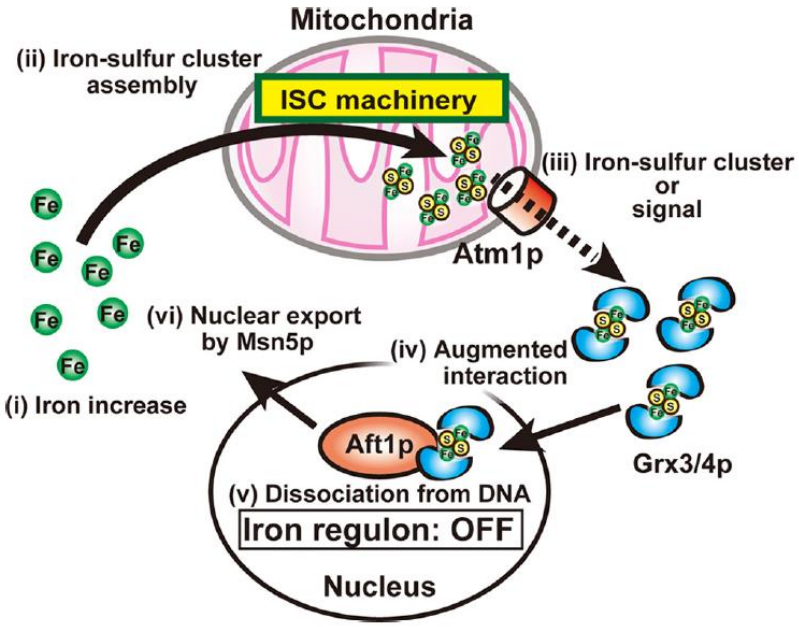

Figure 3 – Model proposed for iron sensing by Aft1p. When iron availability increases, the synthesis of Fe-S clusters rises, increasing the association between Fe-S clusters and Grx3/4p. This association results in the interaction of Grx3/4p with Aft1p, resulting in the dissociation of Aft1p from its target gene promoters and consequently in the exportation of Aft1p to the cytosol. On the other hand, during iron starvation, the synthesis of Fe-S clusters declines, the interaction of Grx3/4p with Aft1p decreases which allows Aft1p to associate to its target genes increasing the transcription of the iron regulon [53].

Nuclear export of the transcription factors Crz1p, Pho4p, and Mig1p, is also mediated by Msn5p, and is regulated by phosphorylation/dephosphorylation mechanisms [58–60]. Phosphorylation of serine residues within the Msn5p-interacting region of Mig1p by the

Snf1p kinase is critical for the glucose-induced nuclear export of Mig1p [60]. Snf1p is involved in the induction of Aft1p target genes at the diauxic shift in response to glucose exhaustion [61]. It was also observed that Aft1p is phosphorylated during the diauxic transition, however Snf1p is not responsible for this phosphorylation. Moreover, the activity of Aft1p is normally regulated by iron in *snf1*Δ cells, since in response to iron deprivation *FET3* is still induced. Besides that, neither S210 or S224 residues of Aft1p are Snf1p phosphorylation sites [62].

1.1.6. High iron-sensing transcriptional activator Yap5p

Yeast can also respond to high iron conditions through the activation of Yap5p [63]. Yap5p is a member of the basic-region leucine zipper transcription factors involved in stress response [64]. Under high iron conditions, Yap5p induce the transcription of *CCC1*, *GRX4*, and *TYW1* [65,66]. Induction of *CCC1*, as mentioned above, results in the import of iron into the vacuole in order to decrease the cytosolic iron pool. However, iron-dependent regulation of *CCC1* is not exclusive to Yap5p, since *CCC1* expression is still stimulated by an unknown iron-responsive regulator in *yap5*Δ cells. Induction of *GRX4* may similarly act as iron sink via increased Fe/S cluster binding, in addition to ensuring efficient Aft1p inhibition during iron sufficiency. Tyw1p is a Fe/S cluster binding involved in the synthesis of modified tRNAs. Tyw1p also helps to prevent iron toxicity by sequestering iron as protein-bound Fe/S clusters. Little is known about the signal involved in Yap5p activation, but the signal of Fe/S clusters availability seems to be important, as in Aft1p regulation, since cells with defects in the mitochondrial Fe/S assembly machinery are unable to induce genes controlled by Yap5p in high iron conditions [67].

1.2. Isc1p and iron homeostasis

1.2.1. Isc1p in sphingolipids metabolism

Sphingolipids are classified as lipids composed of a sphingoid base or long-chain base (LCB - the 18-carbon amino alcohol sphingosine, or one of its derivatives) that can be acylated with to one fatty acid by an amide bond at C2 to produce Ceramide (Cer). Complex sphingolipids are generated when a polar head group (a phosphoalcohol or a sugar residue) is added at C1. There are three main classes of sphingoid bases: sphingosine (Sph),

dihydrosphingosine or sphinganine (dhSph) and phytosphingosine (phytoSph). Fatty acid can be saturated or unsaturated and may differ in carbon number [68,69].

Sphingolipids are prime lipid components of eukaryotic membranes and are particularly abundant in the plasma membrane. Initially they were considered molecules with an exclusively structural role in membranes. However, nowadays it is known that sphingolipids also act as messengers in signalling pathways controlling many cellular processes such as oxidative stress, life span, apoptosis, and cell cycle [70–74].

Sphingolipid metabolism is highly complex and subtle changes in relative amounts of sphingolipid species results in different functional consequences. Ceramide is considered as a "hub" in sphingolipid metabolism. Phytoceramide (phytoCer) is assumed to be the yeast equivalent of the mammalian Cer and the pathways involved in the metabolism of sphingolipids and corresponding enzymes are highly conserved between yeast and higher eukaryotes [75,76].

The *de novo* synthesis of sphingolipids starts in the ER with the condensation of serine and palmitoyl CoA by the serine palmitoyltransferase enzyme to form 3-ketodihydrosphingosine, which is reduced to dhSph by 3'ketodihydrosphingosine reductase. Dihydrosphingosine can be hydroxylated at the C4 position by Sur2p to form phytoSph. Subsequently, ceramide synthase Lag1p and Lac1p catalyse the addition of a fatty acid to phytoSph or dhSph, forming phytoCer and dihydroceramide (dhCer), respectively. PhytoCer also can be generated by hydroxylation of dhCer mediated by Sur2p. After generation of phytoceramides in the ER, they are transported to the Golgi apparatus to form complex sphingolipids that are then sorted to others cellular compartments. Complex sphingolipids are mainly present in the Golgi, vacuole, plasma membrane, and mitochondria (although in much lower levels). Complex sphingolipids are generated by the addition of polar head groups. Addition of phospho-inositol by inositolphosphoceramide synthase (Aur1p and Kei1p) to phytoCer form inositolphosphoceramide (IPC). Inositolphosphoceramide can be then extended with mannose by mannose inositolphosphoceramide synthase (Csg1p, Csg2p and Csh1p) generating mannosylinositol phosphorylceramide (MIPC). Finally, addition of another phospho-inositol residue to MIPC by inositol phosphotransferase leads to the formation of mannose diinositolphosphoceramide ($M(IP)_2C$). Phytoceramide can also be generated by the breakdown of complex sphingolipids. This is catalysed by inositol phosphosphingolipid phospholipase C (Isc1p), which has phospholipase-C-type activity and

hydrolyses the polar head groups from complex sphingolipids, releasing phytoCer and dhCer (Figure 4) [68,69,75,76].

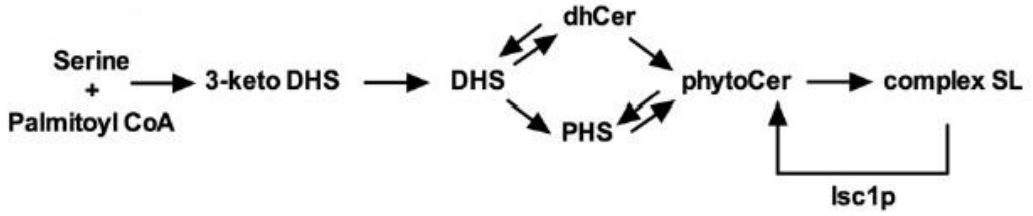

Figure 4 – Schematic representation of sphingolipid metabolism in yeast and the role of the sphingomyelinase Isc1p in the hydrolysis of complex sphingolipids to produce phytoceramide. [(3-keto-DHS - 3- ketodihydrosphingosine); (DHS - dihydrosphingosine); (PHS - phytosphingosine); (dhCer - dihidroceramide); (phytoCer - phytoceramide); (SL - sphingolipids); (Isc1p - inositol phosphosphingolipid phospholipase C)] [68].

Isc1p, encoded by *ISC1*/*YER019w*, is the only known enzyme with phospholipase C activity in *S. cerevisiae* [77]. This enzyme is the yeast homolog of the mammalian neutral sphingomyelinase (nSMase2), sharing 30% of identity to nSMase2. Like nSMase2, its activity depends on the presence of Mg^{2+} and anionic phospholipids as cofactors, such as phosphatidylserine (PS), cardiolipin (CL), and phosphatidylglycerol (PG) and has optimal activity at pH 7.5 [77–79]. Isc1p also has a P-loop-like domain important for substrate binding and/or catalysis, which is conserved in the entire family of SMases [80].

During exponential growth, Isc1p localizes in the ER and in the post-diauxic-shift (PDS) phase is posttranslationally activated and translocated to the outer mitochondrial membrane as an integral membrane protein [81,82]. PS, CL, and PG are almost exclusively present in mitochondria, and their production increases as yeast enters to diauxic shift [78]. It was proposed a "tether-and-pull" model to Isc1p activity, in which PS, CL, and PG bind Isc1p at C terminal, leading to the association of Isc1p at C terminus with the mitochondrial membrane, and consequently, the N-terminal catalytic domain is pushed closer to the membrane to interact with the lipid substrates [79].

Although the concentration of complex sphingolipids in mitochondria is much lower compared, e.g. with the plasma membrane, Isc1p seems to act directly on the complex

sphingolipids found in mitochondria and this is important to mitochondrial function. In the PDS phase, mitochondria were found to be significantly enriched in very long chain α-hydroxylated phytoceramides generated by Isc1p, and the generated ceramide contributes to the normal function of mitochondria [81]. Otherwise, cells lacking Isc1p have an altered mitochondrial lipid profile with a drastic reduction in the levels of α-hydroxylated phytoceramide. The *isc1*Δ cells also exhibit altered sphingolipids levels, mainly, decreased levels of dhSph and most α hydroxylated-phytoceramides, and increased levels of dh-C26-Cer and phyto-C26-Cer [82].

1.2.2. Isc1p in the regulation of iron homeostasis

Studies in our lab allowed the identification of genes differentially expressed in *isc1*Δ cells [74]. Genes found downregulated in the *isc1*Δ mutant are associated with protein biosynthesis and protein fate whereas genes upregulated are related to cell rescue, cell defence, cell transport, transport facilitation, and transport routes. Six genes involved in iron uptake were also identified as being upregulated in *isc1*Δ mutant. These are related with retention of siderophore-iron in the cell wall (*FIT2* and *FIT3*) and transport of siderophore-iron (*ARN1*, *ARN2* /*TAF1*, *ARN3*/*SIT1,* and *ARN4*/*ENB1*). Isc1p-deficient cells also exhibit decreased expression of *GRX3*, which as noted above, is involved in the inactivation of Aft1p when iron is present in sufficient amounts. According to the upregulation of genes involved in iron uptake, it was observed an increase in iron levels of about 2 fold in exponential phase and about 3-4 fold in the PDS phase. The excessive iron may contribute to the higher intracellular oxidation in *isc1*Δ cells, as shown by increased levels of protein carbonylation and lipid peroxidation. Accordingly, cells lacking Isc1p exhibit higher sensitivity to H_2O_2 and decreased chronological lifespan (CLS). The excess of iron was associated to the oxidative stress sensitivity of *isc1*Δ, due to the Fenton reaction of iron with H_2O_2 and consequently production of ROS. When cells were treated with bathophenanthroline dissulfonic acid [(BPS), an iron chelator], the H_2O_2 sensitivity and intracellular oxidation were similar in both *isc1*Δ and parental cells. Although excess iron is associated with oxidative stress sensitivity, and the premature aging of *isc1*Δ is associated with an increase in oxidative stress markers, the decreased CLS does not seem to be due to excessive iron accumulation since

iron chelation does not increase lifespan. On the contrary, treatment with BPS caused a dose-dependent decrease in CLS [74].

Cells lacking Isc1p also exhibit vacuolar fragmentation, abnormal V-ATPase activity and consequently vacuolar pH is more alkaline [83]. As discussed in chapter 1.1.3, pH homeostasis is crucial to iron homeostasis.

Like for the *isc1*Δ mutant, cells with loss of CL exhibit a severe growth defect on non-fermentable carbon sources and deregulation of iron homeostasis. Loss of CL also leads to altered mitochondrial and cellular iron homeostasis, including increased expression of the iron uptake genes, elevated mitochondrial iron levels, and sensitivity to both $FeSO_4$ supplementation and H_2O_2 treatment, probably because defects in Fe/S biogenesis [84,85].

1.2.3. Sphingolipid and iron homeostasis

In addition to the data related to the *isc1Δ* mutant, several lines of evidence suggest a link between sphingolipid signalling and iron homeostasis. Sphingolipid signaling contributes to iron toxicity during iron overload, since reducing sphingolipid synthesis and signaling allow yeast cells to grow in toxic iron conditions. Overexpression of *ORM2* and *ORM1*, two negative regulators of sphingolipid biosynthesis, also rescue the growth defect of *ccc1*Δ cells in high iron conditions. In fact, myriocin treatment, which modulates sphingolipid synthesis through inhibition of serine palmitoyltransferase, allowed wild type (wt) cells to survive in high iron conditions, and *ORM2* deletion, which causes upregulation of sphingolipids synthesis, causes hypersensitivity to subtoxic iron concentrations compared to parental cells [86].

It was observed that high iron conditions increase the levels of LCBs and long-chain base phosphate (LCBPs), resulting in the activation of the Pkh1p/Ypk1p signal transduction cascade, and Ypk1p phosphorylation results in the activation of Smp1p. Deletion of *PKH1*, *YPK1*, or *SMP1* also increases the resistance to high iron. Orm2p overexpression confers resistance to high iron by reducing the levels of LCBs and LCBPs and reducing Ypk1p phosphorylation [86].

Furthermore it was shown that sphingolipids regulate the expression of Fet3p, a multicopper oxidase which, as referred above, is involved in iron transport. Overexpression of Izh2p, which belongs to progestin and adipoQ receptor superfamily, results in the loss of

ability to induce *FET3* expression during iron starvation and PKA (cAMP-dependent protein kinase) is essential for this effect, since in cells lacking Tpk2p (an isoform of PKA), overexpression of Izh2p do not repress *FET3*. Izh2p overexpression represses *FET3* by regulating transcription factors that exert opposing effects on a regulatory element in the *FET3* promoter. Izh2p overexpression results in increased levels of sphingoid bases and repression of *FET3* through the sphingoid base-sensing kinases Pkh1p and Pkh2p. Deletion of either *PKH1* or *PKH2* resulted in the loss of *FET3* repression in response to Izh2p overexpression [87,88].

1.2.4. Isc1p in other cellular processes

Cells lacking Isc1p exhibit some phenotypes associated with mitochondrial dysfunction. Although *isc1*Δ cells do not have major loss of mitochondrial DNA, they are more susceptible to formation of petite colonies, exhibit low activity of the respiratory chain, decreased cytochrome *c* oxidase (COX) activity, mitochondrial hyperpolarization, and mitochondrial fragmentation [82,89–92]. *ISC1* deletion causes growth defects under normal growth conditions, notably at late log and stationary phases and exhibit a strong growth defect in media with non-fermentable carbon sources, such as glycerol, lactate, ethanol or acetate [78,81]. This defect in aerobic respiration at the PDS phase is associated with the incapacity to upregulate genes required for non-fermentable carbon source metabolism [89].

As referred above, *isc1*Δ cells are more sensitive to H_2O_2, and this is associated with an increased accumulation of oxidized proteins and lipids, due a higher intracellular oxidation [74,82]. The premature aging phenotype of *isc1*Δ cells is also associated with increased levels of carbonylation and lipid peroxidation [74]. The higher level of oxidative stress in *isc1*Δ cells was not associated to lower levels of antioxidant defences such as superoxide dismutases (*SOD1* and *SOD2*), cytosolic form of catalase T (*CTT1*) and glutathione levels [74]. However, unlike wt cells, *isc1*Δ cells fail to induce *CTA1* gene expression at PDS phase and therefore exhibit low catalase A (Cta1p) activity. Cta1p is present in mitochondria and peroxisomes, and in wt cells are induced during PDS phase. Overexpression of *CTA1* partially restores the shortened CLS of cells lacking Isc1p, suggesting that Cta1p contributes to the premature aging of *isc1*Δ mutant [89,90,93].

ISC1 deletion also causes sensitivity to high concentrations of salt (NaCl and LiCl), methyl methanesulfonate, and hydroxyurea [94,95]. Isc1p is also involved in heat stress responses, by mediating the production of long and very long chain dihydroceramide species following heat stress [96].

Taken together, these results show that Isc1p plays crucial roles in very important cellular processes, including growth, heat shock response, genotoxic protection, oxidative stress response, aging, mitochondrial function and iron homeostasis.

1.2.5. Pathways involved in *isc1*Δ phenotypes: Sit4p, Hog1p and TORC1-Sch9p

Studies in our lab showed that the mitochondrial dysfunction, oxidative stress sensitivity and shorter lifespan of *isc1*Δ cells are associated with Sit4p, Hog1p and TORC1-Sch9p pathway activation [90–92]. Sit4p is a serine threonine protein phosphatase related to type 2A family of protein phosphatases (PP2A) and has high homology to the human phosphatase PP6. Sit4p is the catalytic subunit of the ceramide-activated protein phosphatase (CAPP), which also contains Tpd3p and Cdc55p as regulatory subunits [97,98]. Sit4p has been involved in cell cycle regulation, ion homeostasis, pH homeostasis, nutrient signalling, endoplasmic reticulum (ER)-Golgi traffic, and in cell wall and actin cytoskeleton organization mediated by Pkc1p [99–103]. Cells lacking Sti4p exhibit de-repression of respiration at logarithmic phase, incapacity to growth in non-fermentative carbon sources such as galactose, ethanol and glycerol, extended longevity and higher resistance to H_2O_2, associated with an increase in antioxidant defences [90,104]. Sit4p is negatively regulated by TORC1, is activated by ceramide and functions downstream of Isc1p [90,105].

In *isc1*Δ cells, higher levels of dh-C26-Cer and phyto-C26-Cer results in Sit4p activation, and Sit4p is a key downstream mediator of the effects of Isc1p deficiency on lifespan, oxidative stress and mitochondrial function. Deletion of *SIT4* in *isc1*Δ cells abolished the premature aging, associated with a decrease in protein carbonylation, and increased H_2O_2 resistance. In fact *isc1*Δ*sit4*Δ cells are more resistant to H_2O_2 and have lower levels of ROS than wt cells, and the levels of protein carbonylation are the same than in parental cells. *SIT4* deletion in *isc1*Δ cells also restores catalase activity, COX activity, the oxygen consumption and cell grown on non-fermentable sources. The double mutant

*isc1*Δ*sit4*Δ also exhibit a normal vacuolar structure, normal ATP-ase activity and consequently normal vacuole pH homeostasis [90 83].

Hog1p also appears to be activated in response to increased ceramide levels displayed by *isc1*Δ cells and contributes to mitochondrial dysfunction, H_2O_2 hypersensitivity and shortened CLS of *isc1*Δ cells [92]. Hog1p, is a mitogen-activated protein kinase (MAPK) involved in the HOG pathway [106]. It is functionally related to mammalian p38 and JNK, two MAPK that are activated by ceramide and contribute to stress-induced cell apoptosis through mitochondrial damage and caspase activation [107–110].

Levels of phospho-Hog1p are increased in *isc1*Δ cells due to increased levels of ceramide. *HOG1* deletion supresses some phenotypes of *isc1*Δ cells, such as the high sensitivity to H_2O_2 associated with a decrease in the accumulation of oxidized proteins, low COX and Cta1p activities, and the incapacity of cells to grow on glycerol medium. The shortened CLS of *isc1*Δ cells is also partially suppressed in *isc1*Δ*hog1*Δ double mutants, associated with a decrease in intracellular oxidation and protein carbonylation [92].

The TORC1-Sch9p pathway is also involved in decreased oxidative stress resistance, mitochondrial function and CLS in *isc1*Δ cells [91]. TORC1 (the rapamycin-sensitive TOR complex 1) contains Lst8p, Kog1p, Tco89p, and either the Ser/Thr protein kinases Tor1p or Tor2p [111]. TORC1 has been associated with the regulation of cell growth acting as a nutrient sensing, autophagy, ribosomal and protein turnover, mitochondrial function, stress response and aging in yeast. Deletion or inhibition of TORC1 with rapamycin extends CLS by an adaptive response that contributes to decrease ROS production in the stationary phase [112–114]. Both protein kinase Sch9p and protein phosphatase Sit4p are identified as TORC1 targets in response to stress and aging. TORC1 is involved in the phosphorylation and activation of Sch9p and in the downregulation of Sit4p. Sch9p and Sit4p can also be activated in response to LCBs and Cer, respectively [90,105,115].

It was observed that in *isc1*Δ cells, Sch9p is hyperphosphorylated in the C-terminus which is mediated by TORC1, indicating an increased TORC1 activity. In fact, *TOR1* or *SCH9* deletion, supressed some phenotypes of *isc1*Δ cells such as hydrogen peroxide sensitivity, premature aging, growth defect on glycerol medium, and defects of both oxygen consumption and COX activity. *TOR1* or *SCH9* deletion also restores the normal tubular mitochondrial network and mitochondrial polarization, partially restores Cta1p expression and decreases ROS levels (although ROS in *isc1*Δ*tor1*Δ and *isc1*Δ*sch9*Δ are higher than in

wt, are lower than in *isc1*Δ). This study also demonstrated that activation of Hog1p in response to ceramide in *isc1*Δ cells is regulated by Sch9p, and deletion of *SCH9* supress *isc1*Δ phenotypes by decreasing Hog1p phosphorylation in *isc1*Δ mutant [91].

Thus, Sit4p, Hog1p and TORC1-Sch9p pathways mediate the effects of Isc1p on lifespan, oxidative stress and mitochondrial function (Figure 5). However, the role of these mediators on the effect of Isc1p in iron regulation remains to be evaluated. Many transcription factors and regulators of iron uptake genes are known, but the signalling pathways that regulate iron homeostasis is still limited.

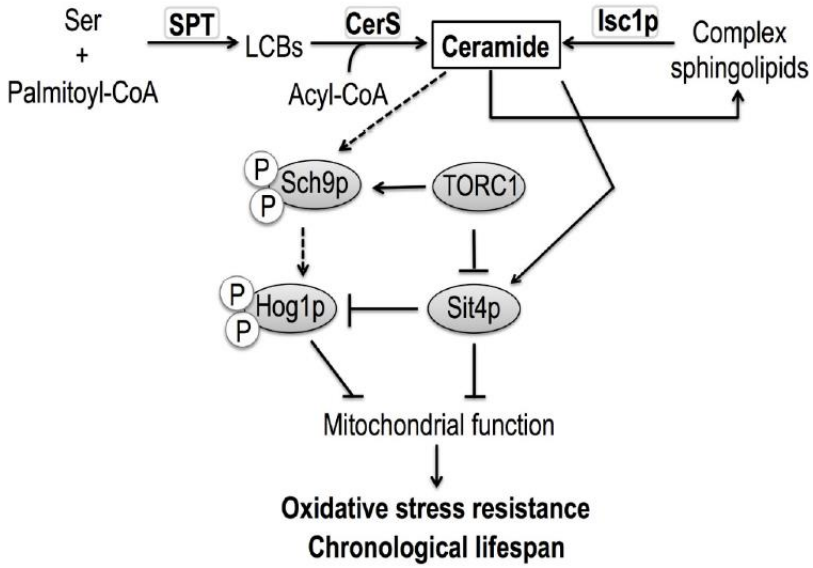

Figure 5 – Cell signalling in response to deletion of *ISC1*. Deletion of *ISC1* results in the activation of Sit4p, Hog1p and TORC1-Sch9p pathways which mediate the effects of Isc1p on mitochondrial function, oxidative stress and lifespan [91].

2. AIMS

Iron is a nutrient needed for many cellular processes and is crucial for the viability of most living organisms. Both iron deficiency and iron overload are detrimental to the cells and have been associated with many pathologies, so the mechanisms of iron metabolism have to be highly regulated in order to maintain iron homeostasis [4]. Previous studies revealed a potential role for Isc1p on the regulation of iron homeostasis in *S. cerevisiae* [74]. Cells lacking Isc1p are characterized by an upregulation of genes involved in iron uptake and increased levels of iron. However, the mechanisms involved in the activation of the iron uptake genes in *isc1*Δ cells are unknown. The objective of this work was to investigate the role of Isc1p in the regulation of iron homeostasis. For that, the profile of accumulation and the oxidation state of the accumulated iron (ferrous and ferric) were characterized along growth. The iron content in different cellular fractions and the distribution of ferric iron *in vivo* using a fluorescent probe were also assessed. In order to identify the molecular mechanisms behind the accumulation of iron in *isc1*Δ cells, the role of Aft1p, the major regulator of iron uptake, was investigated. For that, the accumulation of iron in cells lacking *AFT1* or expressing an inactive Aft1p version and the subcellular localization and phosphorylation status of Aft1p were evaluated. Potential regulatory mechanisms upstream of Aft1p were also addressed.

3. MATERIAL AND METHODS

3.1. Yeast strains, plasmids and growth conditions

S. cerevisiae strains used in this study are listed in Table 1. Yeast cells were grown aerobically at 26°C in a gyratory shaker at 140 rpm, with a ratio of flask volume/medium volume of 5:1. The growth media used were yeast peptone dextrose [YPD, containing 1% (wt/vol) yeast extract (Conda Pronadisa), 2% (wt/vol) bactopeptone (LabM), 2% (wt/vol) glucose (Ficher Scientific)], YPD + Fe [YPD supplemented with 1mM ferrous sulfate (Merck)] and synthetic complete [SC medium, containing drop-out, 2% (wt/vol) glucose (Ficher Scientific), 0.67% (wt/vol) yeast nitrogen base without amino acids (BD BioSciences) and supplemented with appropriate amino acids or nucleotides [0.008% (wt/vol) histidine (Sigma Aldrich), 0.008% (wt/vol) tryptophan (Sigma Aldrich), 0.04% (wt/vol) leucine (Sigma Aldrich) and 0.008% (wt/vol) uracil (Sigma Aldrich)]. For solid medium 2% (wt/vol) agar (Conda Pronadisa) was added.

3.2. Bacteria strains, plasmids and growth conditions

Bacteria strains used in this study are listed in Table 1. Bacteria cells were grown aerobically at 37°C in a gyratory shaker at 180 rpm. The growth media used were lysogeny broth medium supplemented with ampicillin [LB, containing 1% (wt/vol) tryptone (LabM), 1% (wt/vol) NaCl (Merck), 1% (wt/vol) yeast extract (Conda Pronadisa), 0,02% (wt/vol) ampicillin (Sigma Aldrich)]. Solid media were prepared adding 2% (wt/vol) agar (Conda Pronadisa).

3.3. Polymerase chain reaction (PCR)

PCR programs used in this study are described in Table 2. The reaction mix used in each reaction contained 1 x Reaction Buffer (Thermo Scientific), 1.5 mM $MgCl_2$ (Thermo Scientific), 0.2 mM sense primer, 0.2 mM antisense primer, 0.2 μM dNTPs (Thermo Scientific), 1 U Taq Polymerase (Thermo Scientific). For DNA extraction, colony PCR method using the protocol of Murray laboratory was performed [116].

Table 1 - *Saccharomyces cerevisiae* and *Escherichia coli* strains, and plasmids used in this study.

Name	Genotype	Source
S. cerevisiae		
BY4741	Mata, *his3Δ1, leu2Δ0, met15Δ0, ura3Δ0*	EUROSCARF
***isc1*Δ**	BY4741 *isc1*::*KanMx4*	EUROSCARF
***aft1*Δ**	BY4741 *aft1*::*HIS3*	EUROSCARF
***isc1*Δ *aft1*Δ**	BY4741 *isc1*::*KanMx4 aft1*::*HIS3*	This study
***isc1*Δ**	BY4741 *isc1*::*URA3*	This study
***sit4*Δ**	BY4741 *sit4*::*KanMx4*	EUROSCARF
***sit4*Δ *isc1*Δ**	BY4741 *sit4*::*KanMx4 isc1*::*URA3*	[90]
E. coli		
DH5 α	F- endA1 glnV44 thi-1 recA1 relA1 gyrA96 deoR nupG Φ80dlacZΔM15 Δ(lacZYA-argF)U169, hsdR17(rK- mK+), λ–	Lab collection
Plasmids		
p*PEP4-EGFP*	p416ADH-*PEP4*-EGFP	[117]
p*AFT1-HA*	pRS416-*AFT1-HA12*	[52]
p*AFT1-SD-HA*	pRS416-*AFT1-S210,224D-HA12*	[52]
p*AFT1-GFP*	pRS426-*GFP-AFT1*	[56]

3.4. Gene deletion

To create null mutations, yeast cells were transformed with a linear fragment, containing a selectable marker flanked by homologous sequences of the gene, resulting in the replacement of the gene by homologous recombination. These deletion fragments were generated by PCR using the C1000™ Thermal Cycler (Bio-Rad) and analysed by nucleic acid electrophoresis using Tris-acetate-EDTA (TAE) agarose gel 1% (wt/vol) with 0,002% (vol/vol) ethidium bromide. Purification of the products was performed with the Gel Band Purification Kit (GE Healthcare). To create the double mutant BY4741 *isc1*::*KanMx4 aft1*::*HIS3*, the DNA fragment containing the *HIS3* gene and the flanking regions of *AFT1* was amplified from genomic DNA of BY4741 *aft1*::*HIS3* strain and used to transform *isc1*Δ cells. The *URA3* cassette for *ISC1* deletion in BY4741 was amplified from the BY4741 *isc1*::*URA3 sit4*::*KanMx4* background. Al null mutants were confirmed by PCR, using a set of primers

which only amplify when the cassette enters the right place, i.e one primer with homology to the selection marker and the other homologous to the adjacent region of the gene mutated. PCR products were analysed by nucleic acid electrophoresis using TAE agarose gel 1% (wt/vol) with 0,002% (vol/vol) ethidium bromide.

3.5. Yeast transformation

Yeast cells were transformed using the lithium acetate/single-stranded carrier DNA/PEG method as described [118]. Cells in stationary phase were diluted to an OD_{600}=0.2 in YPD medium and were grown until they reach an OD_{600}= 0.8. Once washed, cells were incubated with the transformation mix, containing 240 µL of polyethylene glycol 3350 (PEG 3350) 50% (wt/vol) (Sigma Aldrich), 36 µL of 1.0 M lithium acetate (Sigma Aldrich), 25 µL of single-stranded carrier DNA (2.0 mg ml^{-1}) and the appropriate amount of DNA plus sterile water to a final volume of 360 µL. Afterward, the mixture was incubated during 30 min at 42ºC, for transformation with plasmid DNA. For gene deletion, cells were incubated at 26ºC for 30 min previous to the incubation at 42ºC for 30 min. Finally, cells were harvested, washed and plated on selective SC medium lacking uracil or histidine, depending on the selection marker. Cells incubated in the same conditions but with water instead of DNA were used as negative control.

Table 2 - Primers and PCR programs used in this work.

Gene	Primers	PCR program		
		Annealing temperature (ºC)	Elongation time (sec)	Nº of cycles
aft1*::*HIS3	**AFT1_Amp_Fw** 5´ - TAATTGGGAGTGATAGACGACGA - 3´ **AFT1_Amp_Rv** 5´ - AAAGTCAAAATTGTATAGATGCG - 3´	45.5	110	34
isc1*::*URA3	**ISC1_Amp_Fw** 5´- CTTTCCGCGTAAAAAGGGAA - 3´ **ISC1_Amp_Rv** 5´- TTGCTTTGCATCTATTGACGACG - 3´	50.0	60	34

3.6. Vector amplification

To amplify the plasmid DNA (pDNA), *E. coli* cells carrying the plasmid were inoculated in 5 ml of LB plus ampicillin and incubated overnight at 37°C. The pDNA was extracted using a commercial kit (GenElute Plasmid Miniprep Kit, Sigma Aldrich) and following the instructions of the manual.

To transform *E. coli* cells, pDNA was added to microtubes containing competent DH5α cells, made chemically competent by a calcium soaking protocol [119], and the mixture were incubated on ice for 30 min, followed by 90 sec at 42°C and 2 min on ice. After that, LB was added to a final volume of 1 mL, and cells were incubated at 37°C for 60 min. Finally, cells were plated on selective LB plus ampicillin and incubated overnight at 37°C.

3.7. Iron levels

To quantify total iron levels, yeast cells (6×10^8 cells/mL) were grown to early stationary phase (OD_{600}wt~18, OD_{600}*isc1*Δ~12) in YPD, were washed twice with H_2O, suspended in 0.5 ml of 3% (vol/vol) nitric acid, and incubated 16 h at 98°C. The supernatant (400 µl) was mixed with 160 µl of 38 mg sodium ascorbate ml^{-1} (Sigma Aldrich), 320 µl of 1.7 mg bathophenanthroline disulfonic acid (BPS) ml^{-1} [(Sigma Aldrich), (prepared in ethanol:chloroform, 2:1)], and 126 µl of ammonium acetate [(J. T. Baker), (saturated solution diluted 1:3)]. After mix samples by vortexing and separation of organic and inorganic phases, the organic phase was diluted 20-fold in ethanol:chloroform (2:1). Finally, the absorbance was measured at 535 nm and subtracted the nonspecific absorbance recorded at 680 nm. Iron was quantified by reference to a standard curve using iron sulfate [74,120] . To quantify Fe^{2+}, sodium ascorbate was replaced by water and samples were purged of oxygen by bubbling nitrogen. Fe^{3+} was quantified by subtracting the Fe^{2+} to total iron.

In order to quantify the iron associated with the cell wall, cells were first suspended in digestion buffer [2M sorbitol, 1M phosphate pH 7.5, 0.5M EDTA, 1% (vol/vol) mercaptoethanol] at a concentration of 10 grams cells (wet weight) to 30 ml buffer, with addition of zymolyase (50mg per 10g cells wet weight) and incubated at 37ºC until most of cells have been converted to spheroplasts. After centrifugation for 10 min at 7000 rpm, both supernatant and pellet obtained were collected to a new microtube and nitric acid was added to a final concentration of 3% before incubation at 98°C during 16 h, to quantify the iron associated to the cell wall and to the spheroplasts, respectively.

To perform the quantification of iron in mitochondria, mitochondrial isolation was performed as is described in chapter 3.8, and mitochondria extracts were suspended in 3% nitric acid and incubated at 98°C for the period of 16 h.

Isolation of vacuoles was performed as described [83]. For vacuoles isolation, cells were grown to post-diauxic-shift (PDS) phase in YPD medium, and protein quantification of the vacuolar extracts was performed using the Lowry method .To quantify the iron levels, vacuolar extracts were also suspended in 3% nitric acid and incubated at 98°C for the period of 16 h.

3.8. Mitochondrial isolation

Mitochondrial extracts were performed based on the method described by Daum G, et al. (1982) [121]. Yeast cells grown to the PDS phase in YPD medium were harvested at 5000 rpm for 10 min and washed with deionised water before suspension in digestion buffer [2M sorbitol, 1M phosphate pH 7.5, 0.5M EDTA, and 1% (vol/vol) mercaptoethanol] at a concentration of 10 grams cells (wet weight) to 30 ml buffer with addition of zymolyase (50mg per 10g cells wet weight). Cells were then incubated at 37ºC until most of cells have been converted to spheroplasts. Washed spheroplasts with 1.2M sorbitol were suspended in suspension buffer (0.5M sorbitol, 20mM Tris pH 7.5, 1mM EDTA) and lysed using the Douce homogeneizer. Afterward the suspensions were transferred to small centrifuge flasks and subjected to 3 cycles of 15 min low-speed/high-speed centrifugation (2500 rpm/13000 rpm) and resuspension cycles. The mitochondrial pellet was stored at -80 °C. Protein quantification of the mitochondrial extracts was performed using the Lowry method.

3.9. Chronological lifespan

Chronological lifespan (CLS) was assayed as described [122]. Overnight cultures in YPD medium were diluted to an OD_{600}=0.2 in YPD or YPD + Fe. After 24h (considered time zero, t0), the same volumes of dilutions were plated on YPD medium every two-three days. Colonies were counted after 2-days incubation at 26°C. Cellular viability was expressed as the percentage of the colony-forming units (CFUs) in relation to t0.

3.10. Fluorescence microscopy

In order to evaluate the distribution of ferric iron *in vivo*, BY4741 and *isc1*Δ cells, expressing p*PEP4-GFP* to stain the vacuole, were grown to early stationary phase (OD_{600}wt~18, OD_{600}*isc1*Δ~12) in YPD, and incubated with 20 μM of AL1 [123] (fluorescent probe derived from rhodamine that binds Fe^{3+}) during 3 h. Washed cells with phosphate buffered saline (PBS) were immobilized in agarose beds and observed by fluorescence microscopy (AxioImager Z1, Carl Zeiss).

To assess the localization of Aft1p in wild type (wt) and in *isc1*Δ mutant, cells carrying the plasmid pRS426 *GFP-AFT1* under control of the *AFT1* promoter grown overnight in SC medium lacking uracil were dilute in YPD and grown to an OD_{600}=0.6-2. As positive control, cells were treated with 80 μM of BPS during 4 h, leading to the translocation of Aft1p to the nucleus. To mark the nucleus, PBS washed cells were incubated with 4μg/mL 4'-6-diamidino-2-phenylindole [DAPI, (Molecular Probes, Invitrogen)] during 15 min at room temperature protected from light. Finally, after washing twice with PBS, cells were immobilized in agarose beds and observed by fluorescence microscopy (AxioImager Z1, Carl Zeiss).

Maximum intensity projection of data image stacks was used to output final images using ImageJ 1.45v software [124].

3.11. Western blot analysis

To detect AFT1-HA and AFT1-SD-HA, cells were grown under the same conditions used to grow the cells which were used to quantify iron levels. Cells harbouring the plasmid expressing *AFT1-HA* or *AFT1-SD-HA* under control of the *AFT1* promoter were grown overnight in SC medium lacking uracil and diluted in YPD were they grown to early stationary phase. For protein extraction, cells were harvested, washed and the pellets were suspended in phosphate buffer [50mM KH_2PO_4, 0.1mM EDTA, 1% (vol/vol) Triton, pH7.0] with the addition of zirconia beads. Cells were lysed by vigorous shaking of the cell suspension in the presence of zirconia beads (short pulses of 1 min with 1 min intervals on ice) until majority of cells were lysed. The soluble protein was separated from the cell debris by centrifugation at 13000 rpm for 15 min and the protein concentration was assessed by the Lowry method using bovine serum albumin as a standard. Protein extracts (50 μg) were separated using a 15% SDS polyacrylamide gel at 130 V and transferred to a nitrocellulose

membrane (Hybond-ECL, GE Healthcare) at 160 mA during 1 hour. Membranes were blocked at least for 1 h in TTBS [TBS (Tris-buffered saline) with 0.05% (vol/vol) Tween-20 (Merck)] containing 5 % (wt/vol) dry milk and then incubated overnight with the primary antibody anti-HA (1:200; Santa Cruz). After washing three times with TTBS for 5 min, membranes were incubated with the secondary α-rabbit IgG (1:10000, Sigma-Aldrich) for 1 h and then washed three times with TTBS for 5 min and once with TBS. Immunodetection of bands was revealed by chemiluminescence, using a kit from GE Healthcare.

Aft1p phosphorylation was assessed by differences in electrophoretic run of the protein, since the phosphorylated form exhibit a higher molecular weight than the non-phosphorylated form [52]. Cell lysates were prepared from cells expressing HA-tagged Aft1p grown in YPD media to exponential or stationary phase, and 20 ml or 1 mL of culture were collected, respectively. Pellet obtained after centrifugation was suspended in 400mL of H_2O and 400 mL of 0.2M NaOH, and incubated 5 min at room temperature. After that the mixture were harvested by 13000 rpm at 4ºC during 15 min, and the resulted pellet suspended in sample buffer without 2- mercaptoethanol (2% SDS, 10% glycerol, 0.002% bromphenol blue, 0.0625M Tris HCl) and incubated 5 min at 95ºC. To finish, the suspension was centrifuged by 13000 rpm at 4ºC during 3 min and the supernatant was collected. Protein quantification was performed using the bicinchoninic acid (BCA) assay using bovine serum albumin as a standard. Protein samples (35 µg) were separated using a 6% SDS polyacrylamide gel at 110 V and transferred to a nitrocellulose membrane (Hybond-ECL, GE Healthcare) at 160 mA during 30 min. Membranes were blocked at least for 1 h in TTBS containing 5 % (wt/vol) dry milk and then incubated overnight with the primary antibody anti-HA (1:1500; Santa Cruz). After washing three times with TTBS for 5 min, membranes were incubated with the secondary α-rabbit IgG (1:10000; Sigma-Aldrich) for 1 h and then washed three times with TTBS for 5 min and once with TBS. Immunodetection of bands was revealed by chemiluminescence, using a kit from GE Healthcare.

3.12. Statistical analysis

Data were analysed in GraphPad Prism Software v5.01 (GraphPad Software). Values were compared by one-way ANOVA or two-way ANOVA with Bonferroni correction and by Student's t-test when two groups were analysed *, $p< 0.05$; **, $p< 0.01$; ***, $p< 0.001$; ****, $p<0.0001$

4. RESULTS AND DISCUSSION

4.1. Iron redox speciation and iron distribution in *isc1*Δ cells

4.1.1. Deletion of *ISC1* caused iron accumulation in both exponential and stationary phases of growth

In previous work it was observed that lack of Isc1p leads to an increase in the mRNA levels of genes associated with iron uptake and to an increase in the cellular iron content [74]. Deletion of *ISC1* also resulted in growth defects at the post-diauxic-shift (PDS) phase (Figure 6A) as previous reported, due to the incapacity to upregulate genes required for respiratory metabolism [81,89]. In order to monitor the accumulation of intracellular iron during growth, cells were grown to exponential phase (OD_{600}= 0.6-1) and samples were collected at different time points as represented in the Figure 6A, and iron levels were measured. An increment of around 3-4 fold in iron content of *isc1*Δ cells compared to wild type (wt) cells was observed, and this increment was relatively constant during growth, with a slight decrease (accumulation of about 1.9 fold) at day 11 (Figure 6B). The major difference in the amount of iron (3.7 fold) between wt and *isc1*Δ cells was measured at day 5 (OD_{600}=14 and 16). Significant differences in the amount of iron between the exponential phase and the post-diauxic-shift (PDS) phase were not observed, indicating that iron accumulation in *isc1*Δ cells is not related to a lack of synchronization between iron uptake and cell growth due to the early arrest in growth.

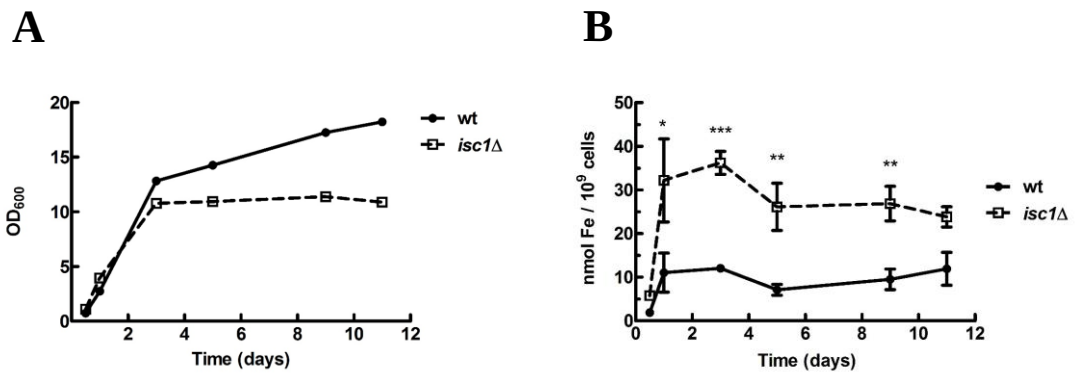

Figure 6 – Cells lacking Isc1p accumulated iron in all phases of growth. A) A representative growth curve of wt cells and *isc1*Δ cells is shown. B) *S. cerevisiae* wt and *isc1*Δ cells were grown on YPD media and iron levels were quantified along growth. Iron levels were expressed as mean values ± SEM of at least three independent experiments. Values were compared by two-way ANOVA, ***, $p < 0.0001$.

4.1.2. Deletion of *ISC1* resulted in the accumulation of both ferric (Fe^{3+}) and ferrous (Fe^{2+}) iron forms

Iron accumulation in *isc1*Δ cells was previously associated with a higher intracellular oxidation and lower resistance to oxidants [74]. This prompted us to analyse the oxidation state of iron along time. It was observed that an initial increment in Fe^{3+} occurs in wt cells until day 1 followed by a decrease until day 5, where Fe^{3+} levels were close to zero (Figure 7A). This is consistent with the fact that respiring cells have less iron associated to the vacuole, and therefore less Fe^{3+}, and less Fe^{3+} species associated with the mitochondria [37,38]. On the other hand, in *isc1*Δ cells the Fe^{3+} levels were constant during growth (Figure 7A) and significantly higher than in wt cells, and both status of iron contribute to iron overload exhibited by *isc1*Δ mutant cells (Figure 7A, 7B).

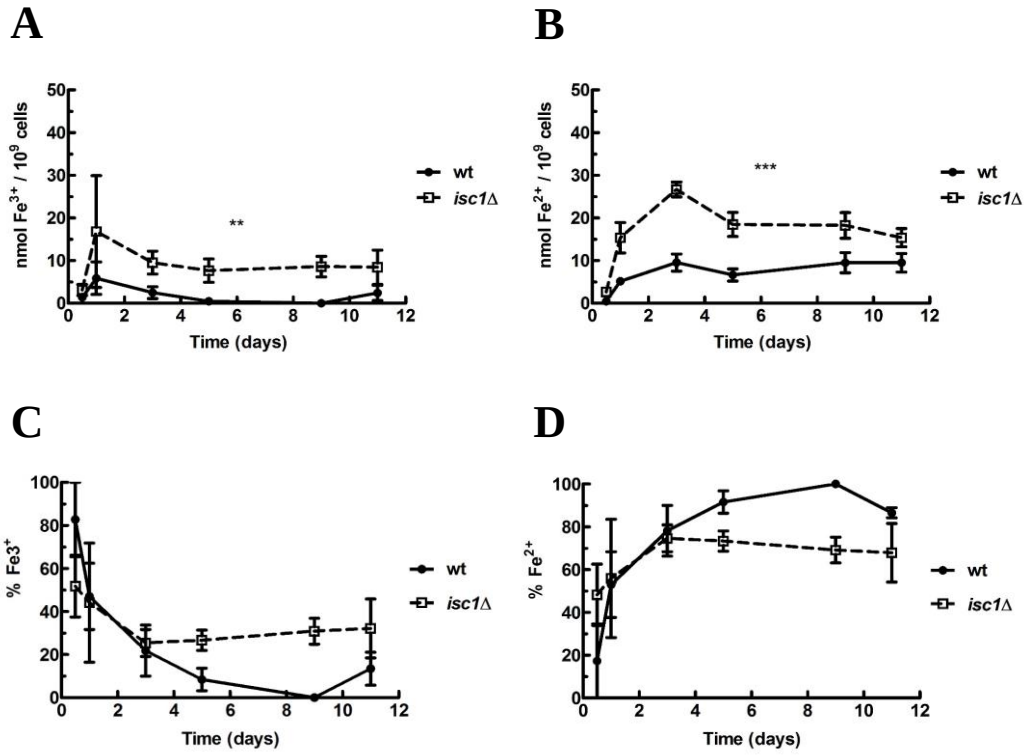

Figure 7 – Cells lacking Isc1p accumulated iron in both oxidation states. A) Fe^{3+} and B) Fe^{2+} levels were quantified in *S. cerevisiae* wt and *isc1*Δ cells during growth on YPD media. C) Fe^{3+} and D) Fe^{2+} levels, expressed as percentage in relation to total iron. Data were expressed as mean values ± SEM of at least three independent experiments. Values were compared by two-way ANOVA, ***, $p < 0.0001$; **, $p < 0.01$.

Analysing the percentage of Fe^{2+} and Fe^{3+} relative to total iron, our results show that *isc1*Δ exhibited a higher percentage of Fe^{3+} and a lesser percentage of Fe^{2+} from PDS phase (day 3, OD=12-14), although it did not reach statistical significance (Figure 7C, 7D). However, when cells were grown in media supplemented with iron, the percentage of Fe^{3+} was significantly higher in *isc1*Δ cells (Figure 8). Both wt cells and *isc1*Δ cells accumulated more iron when grown in media supplemented with iron, however the majority of iron accumulated in wt cells was found in the Fe^{2+} form (25% Fe^{3+}) , while *isc1*Δ cells accumulate a large part (63% Fe^{3+}) in the Fe^{3+} form (Figure 8). This result may indicate that in *isc1*Δ cells iron may be more involved in redox reactions and may be the cause of the high intracellular oxidation reported for this mutant.

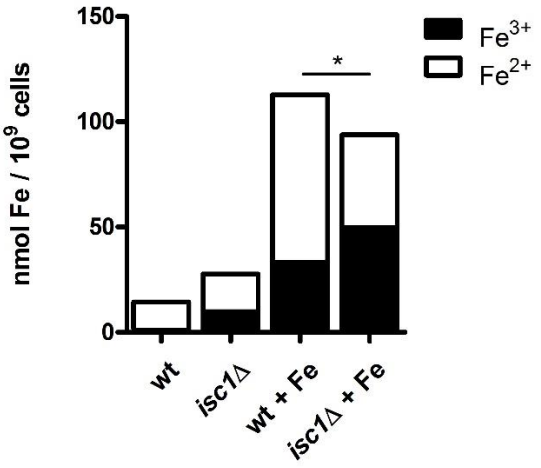

Figure 8 – Cells lacking Isc1p exhibited a higher percentage of Fe^{3+} when grown in medium supplemented with iron. Fe^{3+} and Fe^{2+} levels were quantified in wt and *isc1*Δ cells cultured in YPD (wt, *isc1*Δ) or YPD supplemented with 1mM iron sulphate (wt + Fe, *isc1*Δ + Fe) to early stationary phase (OD_{600}wt~18, OD_{600}*isc1*Δ~12). Data were expressed as mean values (n=8). Values of Fe^{3+} percentage were compared by one-way ANOVA, *, $p< 0.05$.

4.1.3. Iron accumulation in *isc1*Δ cells occured in the cytosol

To assess if iron accumulates in specific compartments in *isc1*Δ cells, we quantified iron levels in the cell wall and the corresponding spheroplasts, in mitochondrial extracts, and in the vacuoles of wt and *isc1*Δ cells.

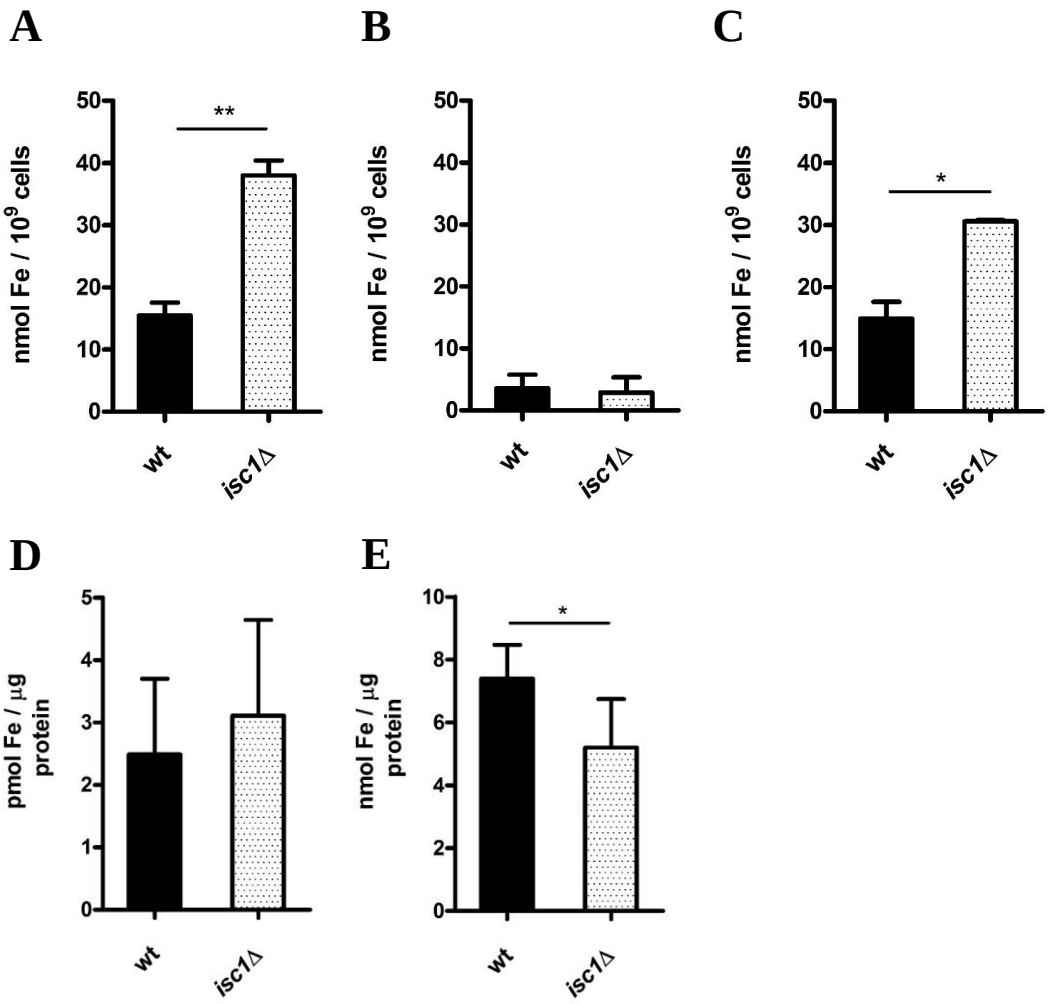

Figure 9 – Cells lacking Isc1p did not accumulate iron in the cell wall neither in the mitochondria and exhibited lower levels of iron associated to the vacuole. Wt and *isc1*Δ cells were grown in YPD to the PDS phase and iron levels were quantified in A) total cellular extracts, B) cell wall, C) spheroplasts, D) mitochondrial extracts, and E) vacuolar extracts. Data were expressed as mean values ± SEM at least three independent experiments. Values were compared by one-way ANOVA, *, $p < 0.05$; **, $p < 0.01$.

The iron associated to the cell wall was investigated since *FIT2* and *FIT3*, which encode proteins involved in retention of siderophore-iron in the cell wall, are upregulated in

*isc1*Δ cells [74]. However, no differences were observed in the content of iron associated to the cell wall between wt and *isc1*Δ cells (Figure 9B). In agreement, excess of iron in *isc1*Δ cells remained in the spheroplasts (Figure 9C). Although upregulation of *FIT2* and *FIT3* could lead to increased levels of iron in the cell wall, in *isc1*Δ cells the membrane transporters involved in the transport of iron-siderophores molecules are also upregulated, which may lead to increased transport of iron into the cells, explaining its lack of accumulation in the cell wall.

Cells lacking Isc1p exhibit mitochondrial dysfunction and an association between mitochondrial dysfunction and mitochondrial iron accumulation was reported before [125,126]. Furthermore, since mitochondria are an important intracellular destination of iron, the potential accumulation of iron in *isc1*Δ cells was investigated. For that, mitochondrial fractions were collected by differential centrifugation and iron quantified as before. We observed that *ISC1* deletion did not cause mitochondrial iron accumulation (Figure 9D).

Additionally, the iron content of vacuolar extracts was investigated, since vacuoles are an important destination of iron. Moreover, *isc1*Δ cells displayed higher levels of Fe^{3+} and iron in the vacuoles consists predominately of Fe^{3+} ions. Notably, vacuolar extracts of *isc1*Δ cells exhibited lower levels of iron (Figure 9E). These results suggest that *isc1*Δ cells accumulate iron in the cytosol, since mitochondria and vacuoles, which are the main iron destinations in the cell, did not exhibit iron accumulation, in fact vacuoles exhibited even lower levels.

4.1.4. *isc1*Δ cells exhibited Fe^{3+} iron delocalization

In order to confirm that *isc1*Δ cells accumulate iron in the cytosol, the distribution in vivo of Fe^{3+} was evaluated by fluorescence microscopy in wt and *isc1*Δ cells expressing a vacuolar protein (Pep4p) fused to GFP. Stationary phase cells were incubated with 20 μM of AL1, a probe that binds Fe^{3+} [123], for 3 h prior to observation under the microscope. Fe^{3+} distribution in *isc1*Δ cells completely differs from the distribution observed in wt cells. In wt cells, Fe^{3+} was confined to the vacuoles whereas in *isc1*Δ cells Fe^{3+} was distributed throughout the cell (Figure 10), suggesting that it accumulates in the cytosol.

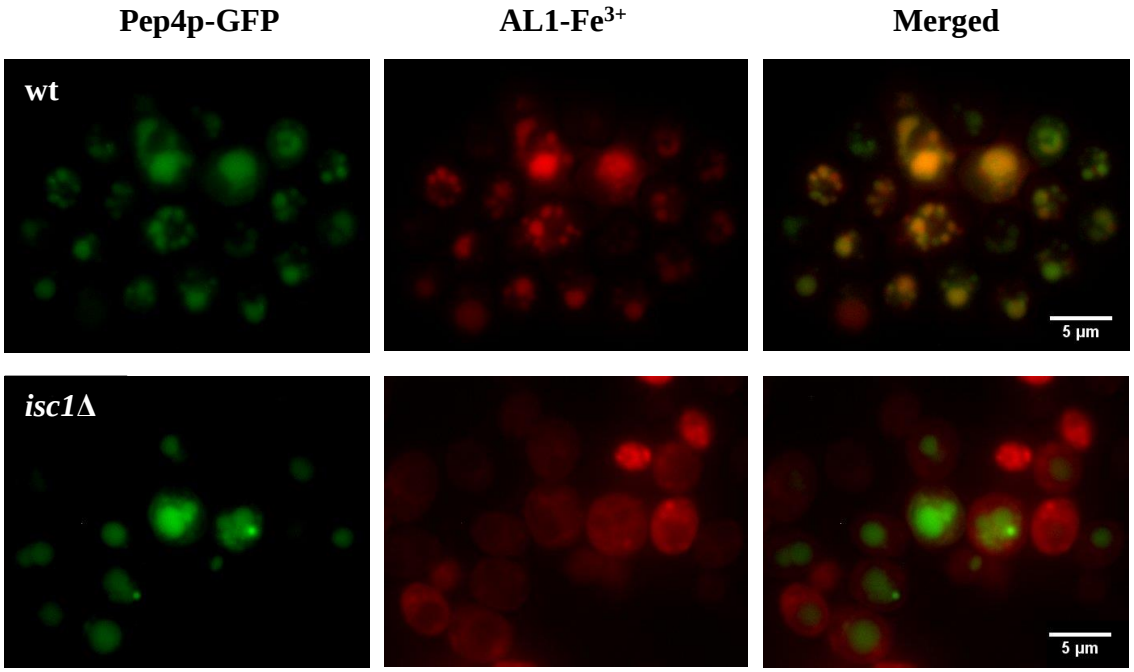

Figure 10 – Fe^{3+} localization was altered in cells lacking Isc1p. Fluorescence photomicrographs showing the distribution of Fe^{3+} in the vacuoles of wt cells and the distribution of Fe^{3+} throughout the cell of *isc1*Δ cells. Cells expressing *PEP4*-GFP, to mark the vacuole, were cultured to early stationary phase and incubated with 20 µM of AL1. Maximum intensity projection was used.

4.2. Role of Aft1p in the accumulation of iron in cells lacking Isc1p

4.2.1. *AFT1* deletion supressed accumulation of iron in *isc1*Δ cells

Aft1p is a key regulator of iron homeostasis, involved in iron uptake under low iron conditions. It was previously suggested that Aft1p is not involved in the induction of iron uptake genes in *isc1*Δ cells based on the fact that the activity of the *CTH2* promoter (using a LacZ reporter) was similar in both wt and *isc1*Δ cells [74]. However, *CTH2* is not a classical Aft1p target and its expression is associated only to prolonged iron deficiency [45] and may not reflect Aft1p activation. To elucidate the involvement of Aft1p in the iron overload of *isc1*Δ mutant, we measured the iron levels in a double mutant *isc1*Δ*aft1*Δ. Deletion of *AFT1* abolished the accumulation of iron in *isc1*Δ cells (Figure 11), indicating that Aft1p is involved in the accumulation of iron in cells lacking Isc1p.

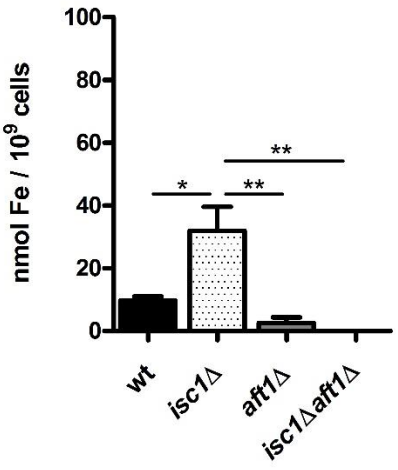

Figure 11 – Deletion of *AFT1* abolished the accumulation of iron in cells lacking Isc1p. *S. cerevisiae* wt, *isc1*Δ, *aft1*Δ and *isc1*Δ*aft1*Δ cells were grown to early stationary phase and iron levels were quantified spectrometrically. Data were expressed as mean values ± SEM of three independent experiments. Values were compared by one-way ANOVA, *, $p<0.05$; **, $p< 0.01$.

4.2.2. *AFT1* deletion decreased the cellular growth of *isc1*Δ cells

Iron overload in *isc1*Δ cells was associated with higher intracellular oxidation, and iron chelation by treatment with bathophenanthroline disulfonic acid (BPS) decreased the oxidative stress sensitivity and ROS production [74]. The double mutant *isc1*Δ*aft1*Δ did not exhibit iron overload, so it was assessed if *AFT1* deletion could improve the growth of *isc1*Δ cells. Consistent with the growth defect at late log and stationary phases previous reported [81], *isc1*Δ cells were unable to achieve optical densities higher than ~13 in rich medium (Figure 12A). *AFT1* deletion *per si* has a negative effect on cellular growth, mainly at exponential phase. Still, *aft1*Δ cells reached the same optical density as wt cells. *AFT1* deletion however, though abolishing iron accumulation in *isc1*Δ cells, did not improve the growth of *isc1*Δ cells (Figure 12A). On the contrary, *isc1*Δ*aft1*Δ cells exhibited a lower growth rate than *isc1*Δ cells. This led us to raise the hypothesis that iron accumulation in *isc1*Δ cells could be a compensatory effect. This was supported by the report that chelating iron by treating cells with BPS caused a dose-dependent decrease in *isc1*Δ mutant chronological lifespan (CLS) [74]. To test this hypothesis, cells were grown in media supplemented with iron and CLS was determined. However, our results showed that iron supplementation did not increase the chronological lifespan (Figure12B).

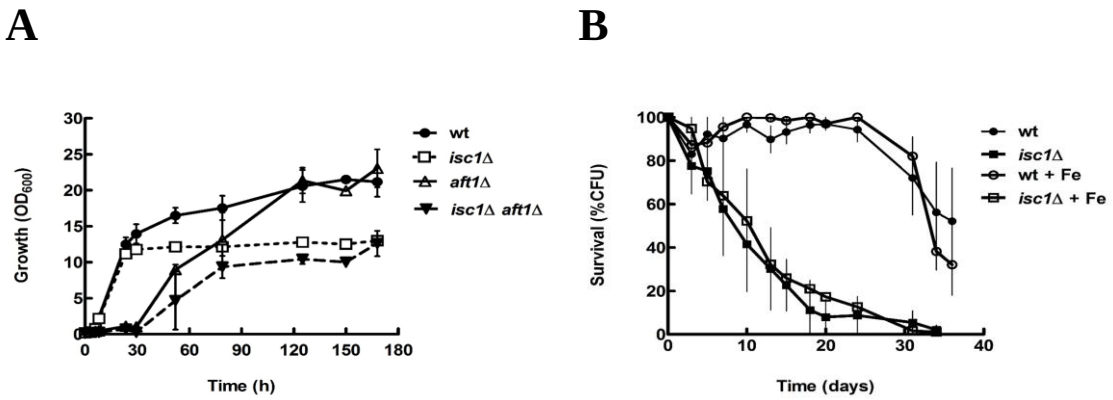

Figure 12 – *AFT1* deletion aggravated the growth rate of *isc1*Δ cells and iron supplementation did not increase the chronological lifespan of *isc1*Δ cells. A) The growth rate of wt, *isc1*Δ, *aft1*Δ, and *isc1*Δ*aft1*Δ cells in YPD medium was monitored by OD_{600} measurements over time. Values are mean ± SEM (n=4). The effect on growth for *isc1*Δ vs *isc1*Δ*aft1*Δ was compared by two-way ANOVA, and was significant (***, $p<0.001$) between the 23-52 h of growth. B) For chronological lifespan, cultures were grown and maintained in YPD (wt, *isc1*Δ) or YPD supplemented with 1mM iron sulfate (wt + Fe, *isc1*Δ + Fe) overtime. The cellular viability was expressed as the percentage of the colony-forming units (CFUs) (in relation to t0). Data were expressed as mean values ± SEM (n=3)

4.2.3. Nuclear localization of Aft1p was higher in *isc1*Δ cells

In response to iron deprivation, Aft1p localizes in nucleus where it activates the transcription of the iron regulon, leading to the uptake of iron and mobilization of iron from intracellular stores. On the other hand, when iron is present in sufficient amounts, Aft1p is translocated to the cytosol [49]. Cells lacking Isc1p exhibit iron overload which is abolished by *AFT1* deletion. To confirm the involvement of Aft1p in the iron accumulation of *isc1*Δ cells, the subcellular localization of Aft1p was assessed. For that, *aft1*Δ and *isc1*Δ*aft1*Δ cells expressing *AFT1-GFP* were grown to exponential phase and visualized by fluorescence microscopy (Figure 13A). In the conditions used, the percentage of cells showing Aft1p-GFP in the nucleus was 48% for the *isc1*Δ mutant and 16% in wt cells. The higher amount of Aft1p-GFP in the nucleus of the *isc1*Δ mutant supports the hypothesis that Aft1p may be active in this mutant even in iron replete conditions (Figure 13B).

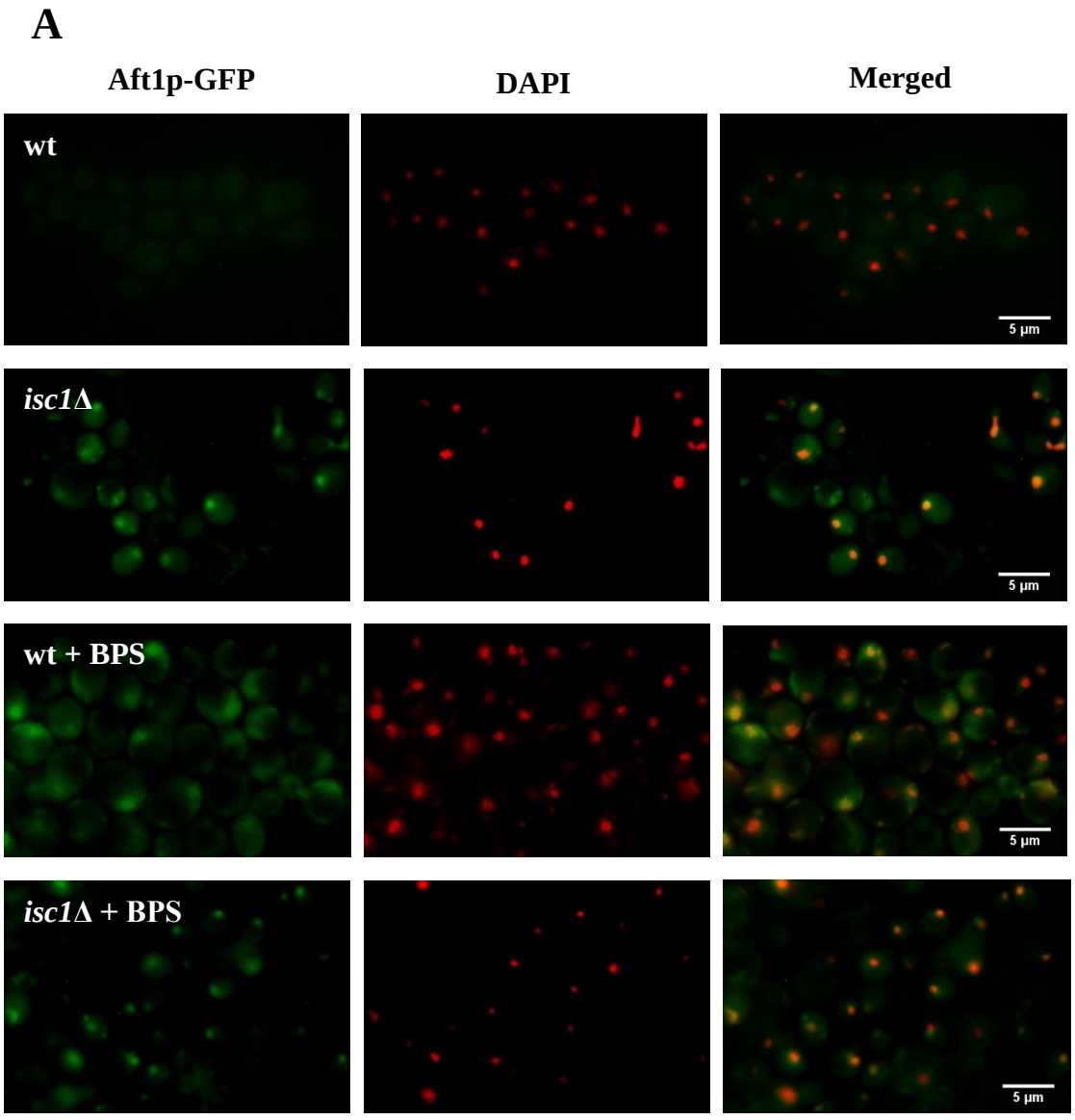

Figure 13 – *ISC1* deletion leads to the translocation of Aft1p to the nucleus. A) Fluorescence photomicrographs showing the subcellular localization of Aft1p (using a GFP-tagged Aft1) in wt and *isc1*Δ cells grown to exponential phase in YPD. Cells treated with BPS, to induce the iron deprivation response, were used as positive control. DAPI staining was used to mark the nucleus. B) The quantification of the percentage of cells showing Aft1-GFP in the nucleus is presented (n=3); t test, *p< 0.05.

4.2.4. *ISC1* deletion caused Aft1p dephosphorylation

Aft1p is posttranlationally modified and this is important for its regulation and translocation between the cytosol and the nucleus in response to iron status [52,53]. Phosphorylation of S210 and S224 residues was identified as essential for the nuclear export of Aft1p in iron replete conditions. In cells expressing a phosphoresistant double mutant (Aft1p-SA), in which serine residues S210 and S224 were replaced with alanines, Aft1p is always localized in the nucleus even in the presence of excess iron [52]. Because *isc1*Δ mutant exhibits a higher Aft1p nuclear localization, we questioned whether this could be due to a decrease in Aft1p phosphorylation. Phosphorylation status of Aft1p can be assessed by analysing the mobility of Aft1p on SDS-PAGE [52]. The non-phosphorylated form of Aft1p is detected at a lower molecular weight than the phosphorylated form. Protein samples from cells expressing an HA-tagged Aft1p, grown in YPD media to exponential or stationary phase, were separated in a 6% SDS polyacrylamide gel and examined by Western blotting using an anti-HA antibody. Our results showed that Aft1p is less phosphorylated in the *isc1*Δ mutant than in the wt cells, more evident in the logarithmic phase (Figure 14). This decrease in Aft1p phosphorylation is the *isc1*Δ mutant is in agreement with the observed higher percentage of Aft1p in the nucleus.

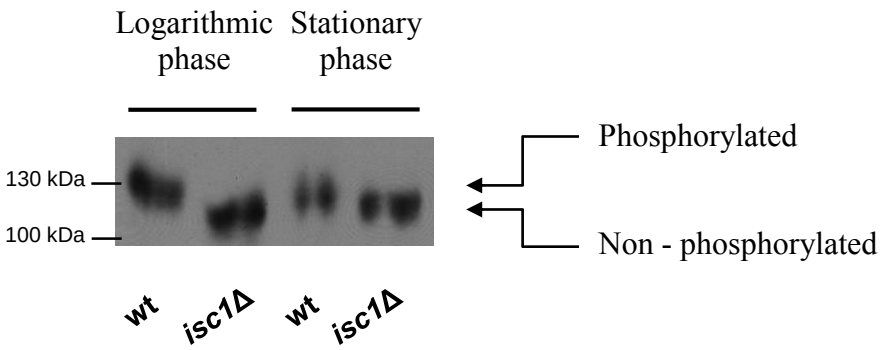

Figure 14 - Aft1p was less phosphorylated in the *isc1*Δ mutant than in wt cells. Proteins samples from *aft1*Δ and *isc1*Δ*aft1*Δ cells expressing Aft1p-HA grown to exponential phase or early stationary phase in YPD were separated by 6% SDS-PAGE. Aft1p was detected by immunoblotting with an anti-HA.

To support the hypothesis that dephosphorylation of Aft1p is responsible for the iron overload observed in *isc1*Δ cells, iron levels were quantified in cells expressing a

phosphomimetic mutant (Aft1p-SD), in which serine residues S210 and S224 were replaced with phosphomimetic aspartates. As expected, expression of the phosphomimetic form of Aft1p significantly decreased the iron content of *isc1*Δ cells to wt levels (Figure 15).

Overall, these results suggest that the high amount of iron in the *isc1*Δ mutant is due to an activation of Aft1p in iron replete conditions due to a decrease in the phosphorylation of the regulatory residues.

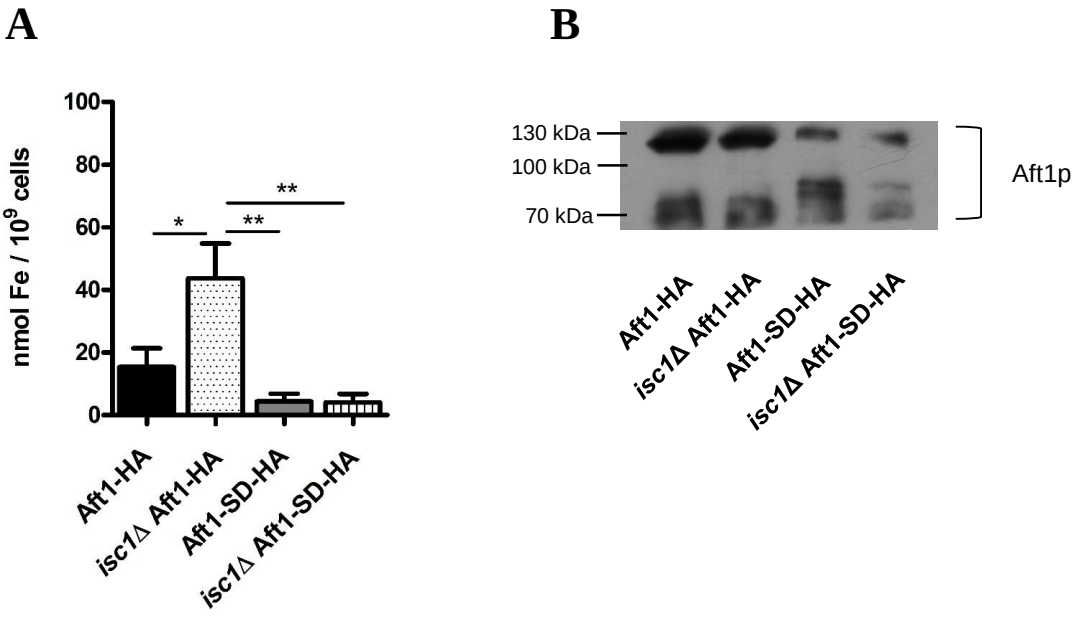

Figure 15 – Expression of a phosphomimetic form of Aft1p abolished iron overload of cells lacking Isc1p. *S. cerevisiae aft1*Δ and *isc1*Δ*aft1*Δ cells expressing Aft1-HA or Aft1-SD-HA were cultured to early stationary phase on YPD medium. A) Iron levels were quantified and B) to confirm the expression of Aft1-HA and Aft1-SD-HA protein samples were separated by 15% SDS-PAGE and Aft1p was detected by immunoblotting with an anti-HA. Iron levels were expressed as mean values ± SEM of four independent experiments. Values were compared by one-way ANOVA, *, $p< 0.05$; **, $p< 0.01$.

4.3. Role of Sit4p in the accumulation of iron in cells lacking Isc1p

4.3.1. *SIT4* deletion did not restore iron levels of *isc1*Δ cells

Sit4p is a protein phosphatase that was found to be hyperactivated in *isc1*Δ cells. Furthermore, Sit4p acts as key downstream mediator of the effects of *isc1*Δ on lifespan, oxidative stress and mitochondrial function [90]. This lead us to raise the hypothesis that Sit4p

could be involved in the dephosphorylation of Aft1p and activation of the iron regulon in *isc1*Δ cells. To test this, iron levels were measured upon *SIT4* deletion. However, deletion of *SIT4* in *isc1*Δ cells did not abolish iron accumulation (Figure 16A), though it appears to revert the increased amount of Fe^{3+} (described before) observed for the *isc1*Δ cells (Figure 16B). Surprisingly, the *sit4*Δ mutant also exhibits iron accumulation (Figure 16A). This may be due to the de-repression of respiration in the *sit4*Δ mutant [90,104] since iron is an essential cofactor of cellular respiration [1,2]. Since Sit4p is involved in the regulation of ion homeostasis and pH and overexpression of Sit4p results in a more alkaline pH than wt cells [100], **A** ccumulation in *sit4*Δ cells may result from ch **B** in pH homeostasis. Indeed, the deletion of *SIT4* may result in a more acidic pH, and there is evidence that iron availability is higher at lower pH [26,29,127].

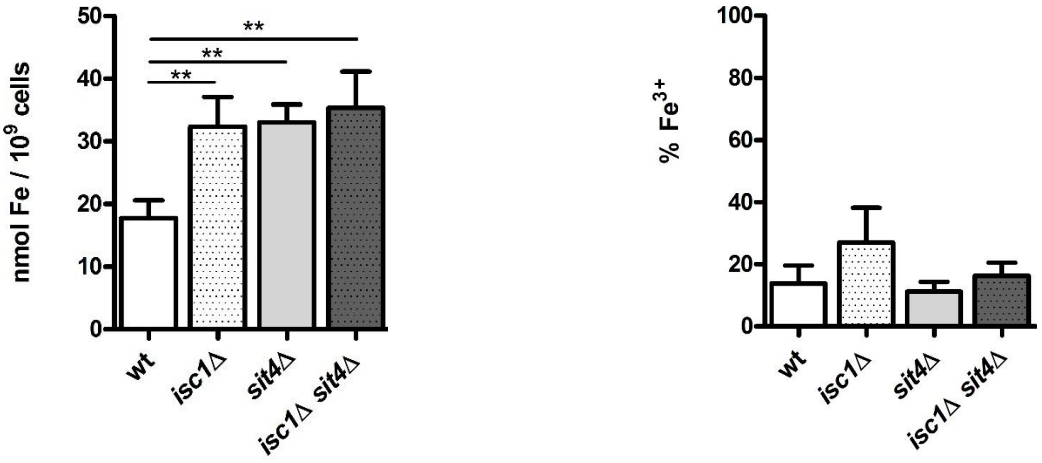

Figure 16 – Deletion of *SIT4* did not abolish iron overload of cells lacking Isc1p. *S. cerevisiae* BY4741, *isc1*Δ, *sit4*Δ, and *isc1*Δ*sit4*Δ cells were grown to early stationary phase on YPD media. A) Quantification of total iron levels and B) Fe^{3+} levels. Data were expressed as mean values ± SEM of six independent experiments. Values were compared by one-way ANOVA, **, $p < 0.01$.

5. CONCLUSIONS AND FUTURE PERSPECTIVES

The sphingomyelinase Isc1p hydrolyses complex sphingolipids to produce ceramide, a bioactive sphingolipid [68,75]. Cells lacking Isc1p have an altered mitochondrial lipid profile with a drastic reduction in the levels of α-hydroxylated phytoceramide, and also exhibit altered sphingolipids levels, namely decreased levels of dihydrosphingosine and most α hydroxylated-phytoceramides, and increased levels of dh-C26-Cer and phyto-C26-Cer [82,90]. Isc1p is involved on lifespan, oxidative stress, mitochondrial function, cell growth, heat shock response, and genotoxic protection [128]. Isc1p has also been associated with iron homeostasis [74]. *ISC1* deletion is characterized by an upregulation of genes involved in iron uptake even under iron replete conditions and consequently iron overload [74]. In the present study, we further investigated the role of Isc1p in the regulation of iron homeostasis.

ISC1 deletion caused an increment of around 3-4 fold in the cellular iron content compared to wt cells (Figure 6A), and both Fe^{2+} and Fe^{3+} forms of iron contribute to this increase. The iron content of *isc1*Δ cells is relatively constant along growth, suggesting that the early growth arrest of *isc1*Δ cells does not contribute to the increase in iron levels. In wt cells, the levels of iron are also relatively constant, but the relative content of Fe^{2+} and Fe^{3+} changed during growth. The percentage of Fe^{3+} was higher in the early stages of growth, but in the post-diauxic-shift (PDS) phase the levels of Fe^{3+} decreased. However, in *isc1*Δ cells it was not observed a decrease in the levels of Fe^{3+} in the PDS phase. This may be explained by the compromised respiratory growth in *isc1*Δ cells, resulting in an increment in the percentage of Fe^{3+} in *isc1*Δ cells compared to wt cells. This increase was significantly higher when cells were grown in media supplemented 1mM iron sulphate. *ISC1* deletion leads to iron accumulation, but iron may not be used by the *isc1*Δ mutant because of the defect exhibited in the aerobic respiration [78,81] associated with a decreased expression of mitochondrial proteins involved in cellular respiration and metabolism, including cytochrome *c* oxidase [90].

The major pool of Fe^{3+} is found in the vacuoles [28], however vacuolar extracts of *isc1*Δ cells exhibited a lower level of iron, and the analysis of the distribution of Fe^{3+} in vivo revealed that Fe^{3+} localization is altered in *isc1*Δ cells. In wt cells Fe^{3+} is localized in the vacuole, consistent with the previous report that vacuoles have a pool of Fe^{3+} [28], whereas in *isc1*Δ cells Fe^{3+} is distributed throughout the cell. These results could be explained by the

higher Aft1p activation, since Aft1p induces the expression of the iron transport systems found in the vacuolar membrane that could lead to increased iron export from the vacuole [22]. Alternatively, the defect in vacuolar acidification displayed by *isc1*Δ cells, due to lower vacuolar H+-ATPase (V-ATPase) activity [83], can also contribute to the exportation of iron from the vacuole, since the acidic environment of the vacuole is required to sequester iron [26,29,127].

Deletion of *ISC1* seems to cause accumulation of iron in the cytosol, since iron was not observed to accumulate in the vacuoles, neither in mitochondrial extracts or the cell wall of *isc1*Δ cells. It was reported that siderophores can serve as intracellular iron storage compounds and *S. cerevisiae* cells can accumulate large and stable intracellular pools of ferric ferrichrome in the cytosol [8,129]. Despite cells lacking Isc1p exhibit an upregulation of genes involved in the uptake of iron-siderophores molecules [74] it is more likely that *isc1*Δ cells accumulate Fe^{3+} as free iron and not bound to siderophores, due to the decreased resistance to oxidative stress reported. If this is true, the higher percentage of Fe^{3+} probably result from free Fe^{2+} oxidation through the Fenton reaction and consequently production of ROS, explaining the higher sensitivity to H_2O_2 and higher intracellular oxidation (Figure 17B). However, the identification of the form in which Fe^{3+} accumulates in *isc1*Δ cells is required to confirm this hypothesis.

SIT4 deletion supresses the intracellular oxidation and the higher sensitivity to oxidative stress of *isc1*Δ cells [90]. However, *isc1*Δ*sit4*Δ also exhibited iron accumulation similarly to *isc1*Δ cells. Despite the higher levels of iron in both *isc1*Δ and *isc1*Δ*sit4*Δ mutant cells, deletion of *SIT4* in *isc1*Δ cells appears to revert the increased amount of Fe^{3+} observed in *isc1*Δ cells. Since without iron supplementation the differences obtained did not reach statistical significance, assays using iron supplemented media will be required to confirm this result. Furthermore, preliminary assays suggest that *SIT4* deletion abolished the altered distribution of Fe^{3+} in *isc1*Δ cells and restores the ability to store iron in the vacuoles. In fact, the defective vacuolar acidification and decreased V-ATPase activity exhibited by *isc1*Δ cells are abolished in *isc1*Δ*sit4*Δ double mutants [83]. *SIT4* deletion also restores catalase activity by increasing Cta1p levels and, thus, the capacity to detoxify H_2O_2 [90]. The ability of *isc1*Δ*sit4*Δ cells to sequester iron in the vacuoles and/or the capacity to induce Cta1p could explain the low oxidative stress sensitivity of this mutant despite the iron accumulation. Overexpression of Ccc1p in *isc1*Δ cells, to increase the importation of iron to the vacuole,

might help answer if the inability to store iron in the vacuoles is related to the higher oxidative stress sensitivity of *isc1*Δ cells.

Iron uptake is one of the most critical steps for maintaining cellular iron homeostasis, and is regulated by the low iron sensing transcriptional activator Aft1p and its paralogue Aft2p [45]. These transcription factors are involved in the activation of the iron regulon in response to iron deficiency, in order to meet the cellular needs of iron. Aft1p is found to accumulate in the nucleus where it activates the transcription of the iron regulon in iron scarce conditions and, when iron is present in sufficient amounts, Aft1p is translocated to the cytoplasm preventing iron uptake [49]. Translocation of Aft1p to the cytoplasm in response to the iron status is mediated by Msn5p [52]. When iron is available, Grx3/4p with bound iron-sulfur (Fe/S) clusters bind to Aft1p, inducing the dissociation of Aft1p from its target promoters, leaving Aft1p available for nuclear export by Msn5p [53] (Figure 17A). On the other hand, Aft1p is active in response to low iron conditions, because during iron starvation the assembly of Fe/S in the mitochondria decreases and dimeric Grx3/4p with bound iron-sulfur clusters are minimal. Consequently Grx3/4p binding to Aft1p is attenuated, and Aft1p binds to target promoters to increase the expression of the iron regulon [53]. Here we provided evidence that Aft1p is active in *isc1*Δ cells even in iron normal conditions, consistent with previous observations reporting upregulation of iron uptake genes and iron overload. Cells lacking Isc1p exhibit higher amount of Aft1p-GFP in the nucleus and *AFT1* deletion or expression of an inactive Aft1p version supresses the accumulation of iron in *isc1*Δ cells. Cells lacking Isc1p exhibit decreased expression of *GRX3* [74], however this is unlikely to be the cause of Aft1p activation in the *isc1*Δ mutant, since it was reported that Grx4p can compensate for the absence of Grx3p [53]. In cells lacking Grx3p or Grx4p, Aft1p is dissociated from target promoters in response to iron repletion as observed in wt cells. Only the deletion of both *GRX3* and *GRX4* results in the Aft1p activation even in iron replete conditions.

In the present study it was also demonstrated that *ISC1* deletion results in a decrease in the phosphorylation of Aft1p and the dephosphorylation of Aft1p is involved in its activation in *isc1*Δ cells. This is supported by the significantly decrease in the iron content of *isc1*Δ cells expressing the phosphomimetic mutant Aft1p-SD to levels similar to wt cells. These results demonstrate that dephosphorylation of Aft1p is the factor behind the accumulation of iron in the *isc1*Δ mutant. However, it was reported that the

dephosphorylation of the residues S210 and 224 per se is not sufficient to constitutively activate Aft1p, since in cells expressing the phosphoresistent mutant, Aft1p does not activate the genes of the iron regulon under iron replete conditions, despite its permanent location in the nucleus [52,53]. This suggests that in addition to the dephosphorylation of Aft1p, other signal, the downregulation of Grx3p or other, involved in the activation of Aft1p is also active (Figure 17B).

How the lack of Isc1p induces Aft1p dephosphorylation remains unknown, and identifying the signal behind the activation of Aft1p in *isc1*Δ cells would be important, particularly because the regulation of Aft1p is poorly known. The higher levels of ceramide exhibited by *isc1*Δ cells results in the activation of Sit4p, Hog1p, and in the TORC1-Sch9p pathway [90–92]. The oxidative stress sensitivity, the shorter lifespan, and the mitochondrial dysfunction of *isc1*Δ cells are associated with Sit4p, Hog1p and Sch9p activation in response to increased ceramide levels. Sit4p is a protein phosphatase [97], but its activation does not seem to be related with the decrease in Aft1p phosphorylation in *isc1*Δ cells, since *isc1*Δ*sit4*Δ cells still exhibit iron overload. However it would be necessary to analyse the phosphorylation state of Aft1p in *isc1*Δ*sit4*Δ cells to confirm that Sit4p is not involved in the dephosphorylation of Aft1p.

The mitogen activated protein kinase Hog1p, which is found activated in *isc1*Δ cells [92], is involved in the response to iron availability in *Candida albicans* and *Cryptococcus neoformans* [130,131]. In *Candida albicans*, Hog1p is transiently phosphorylated under high iron concentrations and *HOG1* deletion led to increased levels of components of the reductive iron uptake system in comparison to wt cells, independent of the iron concentration in the media. When the Hog1p pathway is inhibited in *Cryptococcus neoformans*, expression of two ferroxidases in the high-affinity reductive iron uptake pathway is increased and strongly induced upon oxidative and osmotic stresses. This makes Hog1p a potential regulator of iron homeostasis in *S. cerevisiae* and it would be interesting to investigate if altered Hog1p activity is behind Aft1p activation.

The mechanisms behind the upstream activation of Aft1p in *isc1*Δ cells remain unanswered. Cells lacking Isc1p exhibit decreased V-ATPase activity, and it was reported that loss of V-ATPase activity results in the upregulation of the iron uptake genes under the control of Aft1p [29], but this upregulation does not result in iron accumulation. Therefore the

mechanism that leads to iron overload in *isc1*Δ cells may not be due to its low V-ATPase activity, or at least is not the only mechanism involved.

Mitochondrial Fe/S clusters are involved in Aft1p iron dependent regulation, and Fe/S clusters or signals that involved Fe/S clusters were identified as the signal of iron status [54,55]. Defects in proteins in the mitochondrial Fe/S cluster machinery result in the constitutive expression of Aft1p regulated genes. In *crd1*Δ cells, which lacks cardiolipin synthase, the activity of mitochondrial Fe-S enzymes such as aconitase was found reduced and Aft1p activity was increased [85]. Cardiolipin (CL) and phosphatidilglycerol (PG) are important cofactors of Isc1p activity, and in cells with defects on cardiolipin and phosphatidilglycerol synthesis, the growth dependent activation of Isc1p is impaired [78]. CL is essential for the stability of respiratory chain complexes [85], and Isc1p is also involved in the regulation of cytochrome c oxidase levels, and appears to have a role downstream of CL in the regulation of levels of components of the mitochondrial respiratory system [78]. Defects in mitochondrial Fe/S clusters could contribute to Aft1p activation in *isc1*Δ mutant, and therefore it would be important to measure the activity of a representative Fe/S cluster-dependent enzyme like aconitase.

In summary, our data indicates that *ISC1* deletion leads to the accumulation of iron in the cytosol, and the higher levels of iron are constant along growth. Furthermore, this work demonstrated that iron overload in *isc1*Δ cells is due to activation of the transcriptional regulator Aft1p associated with its dephosphorylation.

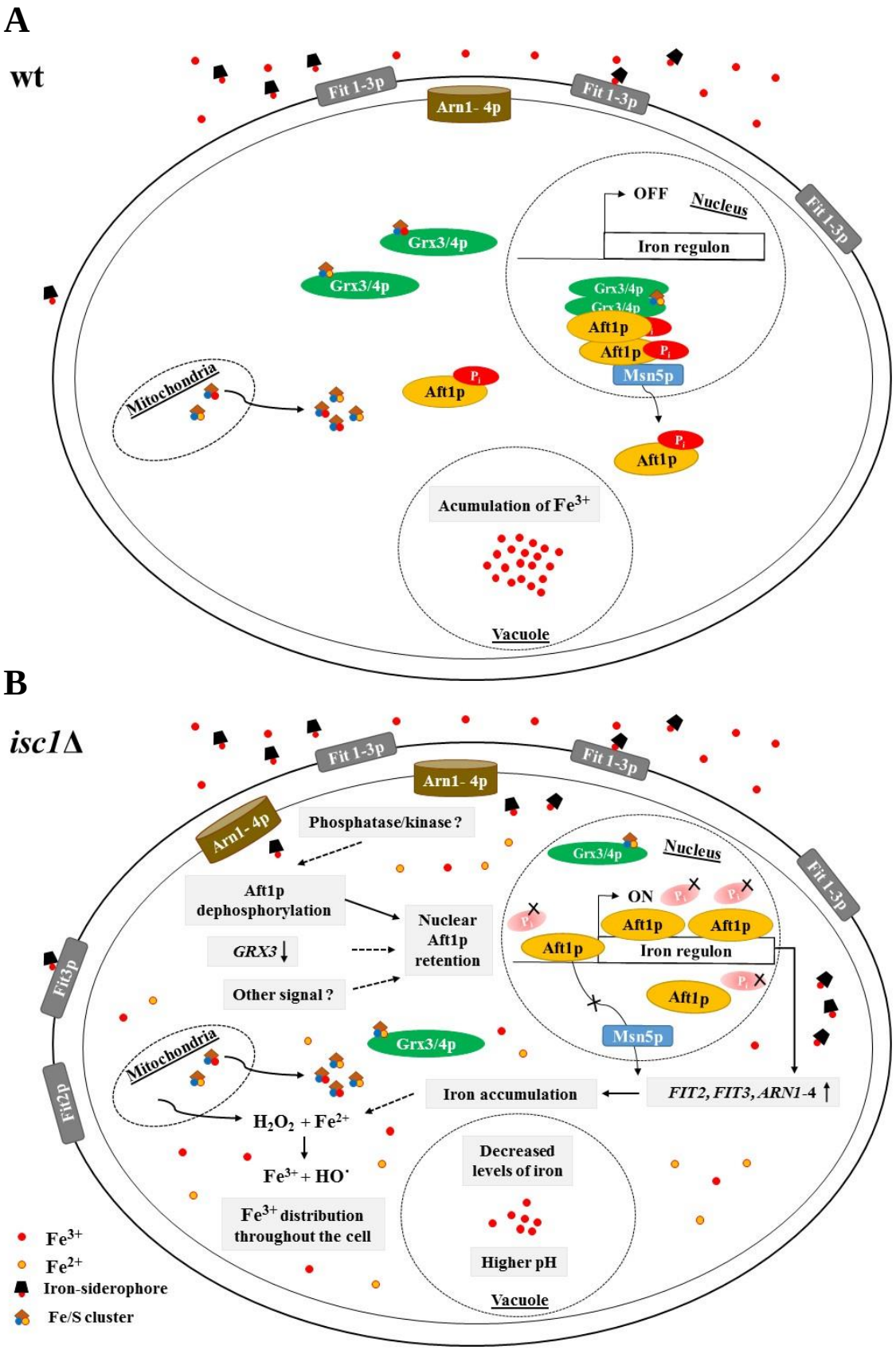
A
wt
Fit 1-3p
Arn1- 4p
Fit 1-3p
Fit 1-3p
OFF
Nucleus
Iron regulon
Grx3/4p
Grx3/4p
Grx3/4p
Aft1p
Aft1p
Msn5p
Mitochondria
Aft1p
Aft1p
Acumulation of Fe3+
Vacuole
B
isc1Δ
Fit 1-3p
Arn1- 4p
Arn1- 4p
Phosphatase/kinase ?
Aft1p dephosphorylation
GRX3
Other signal ?
Nuclear Aft1p retention
Grx3/4p
Nucleus
ON
Aft1p
Aft1p
Aft1p
Iron regulon
Aft1p
Msn5p
Fit 1-3p
Fit3p
Fit2p
Mitochondria
Grx3/4p
Iron accumulation
FIT2, FIT3, ARN1-4
H2O2 + Fe2+
Fe3+ + HO·
Fe3+ distribution throughout the cell
Decreased levels of iron
Higher pH
Vacuole
Fe3+
Fe2+
Iron-siderophore
Fe/S cluster

Figure 17 – Schematic representation for the regulation of the iron regulon by Aft1p in wt and *isc1*Δ cells, under normal iron conditions. A) In wt cells, under normal iron conditions, Grx3/4p with bind Fe/S clusters bound to Aft1p, inducing the dissociation of Aft1p from the iron regulon, and the dimerization of Aft1p allows the recognition of Aft1p by Msn5p, leading to the accumulation of Aft1p in the cytosol, and consequently the expression of the iron regulon is downregulated. B) In *isc1*Δ cells, dephosphorylation of Aft1p, downregulation of Grx3p or other signal, leads to the retention of Aft1p in the nucleus, and to the upregulation of the iron regulon, even under normal iron conditions, resulting in the accumulation of iron in the cytosol. This excessive amount of iron may be involved in the formation of hydroxyl radicals (Fenton reaction) contributing to the oxidative damage observed in *isc1*Δ cells. Additionally, in the *isc1*Δ mutant, vacuoles exhibit lower levels of iron, and Fe^{3+} is found distributed throughout the cell. Decreased levels of iron in the vacuoles upon *ISC1* deletion may be due to the higher exportation of iron from the vacuoles, associated to the increased Aft1p activity, or due to an inability to store iron due to the elevated vacuolar pH of this mutant.

6. REFERENCES

1. Martínez-Pastor, M. T., de Llanos, R., Romero, A. M. & Puig, S. Post-transcriptional regulation of iron homeostasis in *Saccharomyces cerevisiae*. *Int. J. Mol. Sci.* **14,** 15785–15809 (2013).
2. Kaplan, C. D. & Kaplan, J. Iron acquisition and transcriptional regulation. *Chem. Rev.* **109,** 4536–52 (2009).
3. Aisen, P., Enns, C. & Wessling-resnick, M. Chemistry and biology of eukaryotic iron metabolism. *Int. J. Biochem. Cell Biol.* **33,** 940–959 (2001).
4. Papanikolaou, G. & Pantopoulos, K. Iron metabolism and toxicity. *Toxicol. Appl. Pharmacol.* **202,** 199–211 (2005).
5. Ryter, S. W. & Tyrrell, R. M. The heme synthesis and degradation pathways: role in oxidant sensitivity. *Free Radic. Biol. Med.* **28,** 289–309 (2000).
6. Finkel, T. & Holbrook, N. J. Oxidants, oxidative stress and the biology of ageing. *Nature* **408,** 239–247 (2000).
7. Crownover, B. K. & Covey, C. J. Hereditary Hemochromatosis. *Am. Fam. Physician* **87,** 183–190 (2013).
8. Philpott, C. C. Iron uptake in fungi: A system for every source. *Biochim. Biophys. Acta - Mol. Cell Res.* **1763,** 636–645 (2006).
9. Nelissen, B., De Wachter, R. & Goffeau, A. Classification of all putative permeases and other membrane plurispanners of the major facilitator superfamily encoded by the complete genome of *Saccharomyces cerevisiae*. *FEMS Microbiol. Rev.* **21,** 113–134 (1997).
10. Pao, S. S., Paulsen, I. T. & Saier, M. H. Major facilitator superfamily. *Microbiol. Mol. Biol. Rev.* **62,** 1–34 (1998).
11. Heymann, P. & Ernst, J. F. Identification and substrate specificity of a ferrichrome-type siderophore transporter (Arn1p) in *Saccharomyces cerevisiae*. *FEMS Microbiol. Lett.* **186,** 221–227 (2000).
12. Heymann, P., Ernst, J. F. & Winkelmann, G. Identification of a fungal triacetylfusarinine C siderophore transport gene (*TAF1*) in *Saccharomyces cerevisiae* as a member of the major facilitator superfamily. *Biometals* **12,** 301–6 (1999).
13. Lesuisse, E., Simon-casteras, M. & Labbe, P. Siderophore- mediated iron uptake in *Saccharomyces cerevisiae*: the *SIT1* gene encodes a ferrioxamine B permease that belongs to the major facilitator superfamily. *Microbiology* **144,** 3455–3462 (1998).
14. Heymann, P., Ernst, J. F. & Winkelmann, G. A gene of the major facilitator superfamily encodes a transporter for enterobactin (Enb1p) in *Saccharomyces cerevisiae*. *Biometals* **13,** 65–72 (2000).
15. Protchenko, O. *et al.* Three cell wall mannoproteins facilitate the uptake of iron in *Saccharomyces cerevisiae*. *J. Biol. Chem.* **276,** 49244–49250 (2001).
16. Lesuisse, E., Casteras-Simon, M. & Labbe, P. Evidence for the *Saccharomyces cerevisiae* Ferrireductase System Being a Multicomponent Electron Transport Chain. *J. Biol. Chem.* **271,** 13578 –13583 (1996).
17. Askwith, C. *et al.* The *FET3* gene of *S. cerevisiae* encodes a multicopper oxidase required for ferrous iron uptake. *Cell* **76,** 403–410 (1994).
18. Stearman, R., Yuan, D. S., Yamaguchi-Iwai, Y., Klausner, R. D. & Dancis, A. A Permease-Oxidase Complex Involved in High-Affinity Iron Uptake in Yeast. *Science (80-.).* **271,** 1552–1557 (1996).
19. Chen, X.-Z. *et al.* Yeast *SMF1* Mediates H+-coupled Iron Uptake with Concomitant Uncoupled Cation Currents. *J. Biol. Chem.* **274,** 35089–35094 (1999).

20. Dix, D. R., Bridgham, J. T., Broderius, M. A., Byersdorfer, C. A. & Eide, D. J. The *FET4* Gene Encodes the Low Affinity Fe(II) Transport Protein of *Saccharomyces cerevisiae*. *J. Biol. Chem.* **269,** 26092–26099 (1994).

21. Holmes-Hampton, G. P. Biophysical probes of iron metabolism in yeast cells, mitochondria, and mouse brains. *PhD thesis, Texas A&M Univ.* (2012). doi:10.1007/s13398-014-0173-7.2

22. Philpott, C. C. & Protchenko, O. Response to iron deprivation in *Saccharomyces cerevisiae*. *Eukaryot. Cell* **7,** 20–27 (2008).

23. Raguzzi, F., Lesuisse, E. & Crichton, R. R. Iron storage in *Saccharomyces cerevisiae*. *FEBS Lett.* **231,** 253–258 (1988).

24. Li, L., Chen, O. S., Ward, D. M. & Kaplan, J. *CCC*1 Is a Transporter That Mediates Vacuolar Iron Storage in Yeast. *J. Biol. Chem.* **276,** 29515–29519 (2001).

25. Singh, A., Kaur, N. & Kosman, D. J. The Metalloreductase Fre6p in Fe-Efflux from the Yeast Vacuole. *J. Biol. Chem.* **282,** 28619–28626 (2007).

26. Urbanowski, J. L. & Piper, R. C. The iron transporter Fth1p forms a complex with the Fet5 iron oxidase and resides on the vacuolar membrane. *J. Biol. Chem.* **274,** 38061–38070 (1999).

27. Portnoy, M. E., Liu, X. F. & Culotta, V. C. *Saccharomyces cerevisiae* expresses three functionally distinct homologues of the nramp family of metal transporters. *Mol. Cell. Biol.* **20,** 7893–7902 (2000).

28. Cockrell, A. L., Holmes-Hampton, G. P., McCormick, S. P., Chakrabarti, M. & Lindahl, P. A. Mössbauer and EPR study of iron in vacuoles from fermenting *Saccharomyces cerevisiae*. *Biochemistry* **50,** 10275–10283 (2011).

29. Diab, H. I. & Kane, P. M. Loss of Vacuolar H+-ATPase (V-ATPase) Activity in Yeast Generates an Iron Deprivation Signal That Is Moderated by Induction of the Peroxiredoxin TSA2. *J. Biol. Chem.* **288,** 11366–11377 (2013).

30. Froschauer, E. M., Schweyen, R. J. & Wiesenberger, G. The yeast mitochondrial carrier proteins Mrs3p/Mrs4p mediate iron transport across the inner mitochondrial membrane. *Biochim. Biophys. Acta* **1788,** 1044–1050 (2009).

31. Foury, F. & Roganti, T. Deletion of the mitochondrial carrier genes *MRS3* and *MRS4* suppresses mitochondrial iron accumulation in a yeast frataxin-deficient strain. *J. Biol. Chem.* **277,** 24475–24483 (2002).

32. Mühlenhoff, U. *et al.* A Specific Role of the Yeast Mitochondrial Carriers Mrs3/4p in Mitochondrial Iron Acquisition under Iron-limiting Conditions. *J. Biol. Chem.* **278,** 40612–40620 (2003).

33. Froschauer, E. M. *et al.* The mitochondrial carrier Rim2 co-imports pyrimidine nucleotides and iron. *Biochem. J.* **455,** 57–65 (2013).

34. Yoon, H. *et al.* Rim2, a pyrimidine nucleotide exchanger, is needed for iron utilization in mitochondria. *Biochem. J.* **440,** 137–146 (2011).

35. Li, L., Miao, R., Jia, X., Ward, D. M. & Kaplan, J. Expression of the Yeast Cation Diffusion Facilitators Mmt1 and Mmt2 Affects Mitochondrial and Cellular Iron Homeostasis: Evidence for Mitochondrial Iron Export. *J. Biol. Chem.* **289,** 17132–17141 (2014).

36. Li, L. & Kaplan, J. Characterization of two homologous yeast genes that encode mitochondrial iron transporters. *J. Biol. Chem.* **272,** 28485–93 (1997).

37. Holmes-Hampton, G. P. *et al.* A nonheme high-spin ferrous pool in mitochondria isolated from fermenting *Saccharomyces cerevisiae*. *Biochemistry* **49,** 4227–34 (2010).

38. Garber, J. M. *et al.* Biophysical characterization of iron in mitochondria isolated from respiring and fermenting yeast. *Biochemistry* **49,** 5436–5444 (2010).

39. Holmes-hampton, G. P., Jhurry, N. D., Mccormick, S. P. & Lindahl, P. A. Iron Content of *Saccharomyces cerevisiae* Cells Grown under Iron-Deficient and Iron-Overload Conditions. *Biochemistry* **52,** 105–114 (2013).

40. Yamaguchi-Iwai, Y., Dancis, A. & Klausner, R. D. AFT1: a mediator of iron regulated transcriptional control in *Saccharomyces cerevisiae*. *EMBO J.* **14,** 1231–1239 (1995).

41. Blaiseau, P. L., Lesuisse, E. & Camadro, J. M. Aft2p, a novel iron-regulated transcription activator that modulates, with Aft1p, intracellular iron use and resistance to oxidative stress in yeast. *J. Biol. Chem.* **276,** 34221–34226 (2001).

42. Rutherford, J. C., Jaron, S., Ray, E., Brown, P. O. & Winge, D. R. A second iron-regulatory system in yeast independent of Aft1p. *Proc. Natl. Acad. Sci. U. S. A.* **98,** 14322–14327 (2001).

43. Rutherford, J. C., Jaron, S. & Winge, D. R. Aft1p and Aft2p mediate iron-responsive gene expression in yeast through related promoter elements. *J. Biol. Chem.* **278,** 27636–27643 (2003).

44. Courel, M., Lallet, S., Camadro, J. M. & Blaiseau, P. L. Direct activation of genes involved in intracellular iron use by the yeast iron-responsive transcription factor Aft2 without its paralog Aft1. *Mol. Cell. Biol.* **25,** 6760–6771 (2005).

45. Outten, C. E. & Albetel, A. N. Iron sensing and regulation in *Saccharomyces cerevisiae*: Ironing out the mechanistic details. *Curr. Opin. Microbiol.* **16,** 662–668 (2013).

46. Puig, S., Askeland, E. & Thiele, D. J. Coordinated Remodeling of Cellular Metabolism during Iron Deficiency through Targeted mRNA Degradation. *Cell* **120,** 99–110 (2005).

47. Puig, S., Vergara, S. V. & Thiele, D. J. Cooperation of Two mRNA-Binding Proteins Drives Metabolic Adaptation to Iron Deficiency. *Cell Metab.* **7,** 555–564 (2008).

48. Martínez-Pastor, M., Vergara, S. V, Puig, S. & Thiele, D. J. Negative feedback regulation of the yeast *CTH1* and *CTH2* mRNA binding proteins is required for adaptation to iron deficiency and iron supplementation. *Mol. Cell. Biol.* **33,** 2178–2187 (2013).

49. Yamaguchi-Iwai, Y., Ueta, R., Fukunaka, A. & Sasaki, R. Subcellular Localization of Aft1 Transcription Factor Responds to Iron Status in *Saccharomyces cerevisiae*. *J. Biol. Chem.* **277,** 18914–18918 (2002).

50. Ehrensberger, K. M. & Bird, A. J. Hammering out details: Regulating metal levels in eukaryotes. *Trends Biochem. Sci.* **36,** 524–531 (2011).

51. Ueta, R., Fukunaka, A. & Yamaguchi-Iwai, Y. Pse1p mediates the nuclear import of the iron-responsive transcription factor Aft1p in *Saccharomyces cerevisiae*. *J. Biol. Chem.* **278,** 50120–50127 (2003).

52. Ueta, R., Fujiwara, N., Iway, K. & Yamaguchi-iwai, Y. Mechanism Underlying the Iron-dependent Nuclear Export of the Iron-responsive Transcription Factor Aft1p in *Saccharomyces cerevisiae*. *Mol. Biol. Cell* **18,** 2980–2990 (2007).

53. Ueta, R., Fujiwara, N., Iwai, K. & Yamaguchi-Iwai, Y. Iron-Induced Dissociation of the Aft1p Transcriptional Regulator from Target Gene Promoters is an Initial Event in Iron-Dependent Gene Suppression. *Mol. Cell. Biol.* **32,** 4998–5008 (2012).

54. Rutherford, J. C. *et al.* Activation of the Iron Regulon by the Yeast Aft1/Aft2 Transcription Factors Depends on Mitochondrial but Not Cytosolic Iron-Sulfur Protein Biogenesis. *J. Biol. Chem.* **280,** 10135–10140 (2005).

55. Gomez, M. *et al.* Malfunctioning of the Iron–Sulfur Cluster Assembly Machinery in *Saccharomyces cerevisiae* Produces Oxidative Stress via an Iron-Dependent Mechanism, Causing Dysfunction in Respiratory Complexes. *PLoS One* **9,** e111585 (2014).

56. Crisp, R. J. *et al.* Inhibition of Heme Biosynthesis Prevents Transcription of Iron Uptake Genes in Yeast. *J. Biol. Chem.* **278,** 45499–45506 (2003).

57. Leighton, J. & Schatz, G. An ABC transporter in the mitochondrial inner membrane is required for normal growth of yeast. *EMBO J.* **14,** 188–195 (1995).

58. Boustany, L. M. & Cyert, M. S. Calcineurin-dependent regulation of Crz1p nuclear export requires Msn5p and a conserved calcineurin docking site. *Genes Dev.* **16,** 608–619 (2002).

59. Kaffman, A., Rank, N. M., O'Neill, E. M., Huang, L. S. & O'Shea, E. K. The receptor Msn5 exports the phosphorylated transcription factor Pho4 out of the nucleus. *Nature* **396,** 482–486 (1998).

60. DeVit, M. J. & Johnston, M. The nuclear exportin Msn5 is required for nuclear export of the Mig1 glucose repressor of *Saccharomyces cerevisiae*. *Curr. Biol.* **9,** 1231–1241 (1999).

61. Haurie, V., Boucherie, H. & Sagliocco, F. The Snf1 protein kinase controls the induction of genes of the iron uptake pathway at the diauxic shift in *Saccharomyces cerevisiae*. *J. Biol. Chem.* **278,** 45391–45396 (2003).

62. Dale, S., Wilson, W. A., Edelman, A. M. & Hardie, D. G. Similar substrate recognition motifs for mammalian AMP-activated protein kinase, higher plant HMG-CoA reductase kinase-A, yeast *SNF1*, and mammalian calmodulin-dependent protein kinase I. *FEBS Lett.* **361,** 191–195 (1995).

63. Li, L., Bagley, D., Ward, D. M. & Kaplan, J. Yap5 is an iron-responsive transcriptional activator that regulates vacuolar iron storage in yeast. *Mol. Cell. Biol.* **28,** 1326–1337 (2008).

64. Fernandes, L., Rodrigues-Pousada, C. & Struhl, K. Yap, a novel family of eight bZIP proteins in *Saccharomyces cerevisiae* with distinct biological functions. *Mol. Cell. Biol.* **17,** 6982–6993 (1997).

65. Pimentel, C. *et al.* The role of the Yap5 transcription factor in remodeling gene expression in response to Fe bioavailability. *PLoS One* **7,** e37434 (2012).

66. Li, L., Jia, X., Ward, D. M. & Kaplan, J. Yap5 protein-regulated transcription of the *TYW1* gene protects yeast from high iron toxicity. *J. Biol. Chem.* **286,** 38488–38497 (2011).

67. Li, L. *et al.* A role for iron-sulfur clusters in the regulation of transcription factor Yap5-dependent high iron transcriptional responses in yeast. *J. Biol. Chem.* **287,** 35709–35721 (2012).

68. Spincemaille, P., Matmati, N., Hannun, Y. A., Cammue, B. P. A. & Thevissen, K. Sphingolipids and mitochondrial function in budding yeast. *Biochim. Biophys. Acta* **1840,** 3131–3137 (2014).

69. Rego, A. *et al.* The yeast model system as a tool towards the understanding of apoptosis regulation by sphingolipids. *FEMS Yeast Res.* **14,** 160–178 (2014).

70. Epstein, S., Castillon, G. A., Qin, Y. & Riezman, H. An essential function of sphingolipids in yeast cell division. *Mol. Microbiol.* **84,** 1018–1032 (2012).

71. Eisenberg, T. & Büttner, S. Lipids and cell death in yeast. *FEMS Yeast Res.* **14,** 179–197 (2014).

72. Huang, X., Withers, B. R. & Dickson, R. C. Sphingolipids and lifespan regulation. *Biochim. Biophys. Acta - Mol. Cell Biol. Lipids* **1841,** 657–664 (2014).

73. Aerts, A. M. *et al.* Level of M(IP)2C sphingolipid affects plant defensin sensitivity, oxidative stress resistance and chronological life-span in yeast. *FEBS Lett.* **580,** 1903–1907 (2006).

74. Almeida, T. *et al.* Isc1p Plays a Key Role in Hydrogen Peroxide Resistance and Chronological Lifespan through Modulation of Iron Levels and Apoptosis. *Mol. Biol. Cell* **19,** 865–876 (2008).

75. Hannun, Y. A. & Obeid, L. M. Principles of bioactive lipid signalling: lessons from sphingolipids. *Nat. Rev. Mol. Cell Biol.* **9,** 139–150 (2008).

76. Hannun, Y. A. & Obeid, L. M. Many ceramides. *J. Biol. Chem.* **286,** 27855–27862 (2011).

77. Sawai, H. *et al.* Identification of *ISC1* (*YER019w*) as inositol phosphosphingolipid phospholipase C in *Saccharomyces cerevisiae*. *J. Biol. Chem.* **275,** 39793–39798 (2000).

78. Vaena de Avalos, S. *et al.* The phosphatidylglycerol/cardiolipin biosynthetic pathway is required for the activation of inositol phosphosphingolipid phospholipase C, Isc1p, during growth of *Saccharomyces cerevisiae*. *J. Biol. Chem.* **280,** 7170–7177 (2005).

79. Okamoto, Y., Vaena de Avalos, S. & Hannun, Y. A. Structural Requirements for Selective Binding of *ISC1* to Anionic Phospholipids. *J. Biol. Chem.* **277,** 46470–46477 (2002).

80. Okamoto, Y., Vaena de Avalos, S. & Hannun, Y. A. Functional Analysis of *ISC1* by Site-Directed Mutagenesis. *Biochemistry* **42,** 7855–7862 (2003).

81. Vaena de Avalos, S., Okamoto, Y. & Hannun, Y. a. Activation and localization of inositol phosphosphingolipid phospholipase C, Isc1p, to the mitochondria during growth of *Saccharomyces cerevisiae*. *J. Biol. Chem.* **279,** 11537–11545 (2004).

82. Kitagaki, H. *et al.* Isc1 regulates sphingolipid metabolism in yeast mitochondria. *Biochim. Biophys. Acta* **1768,** 2849–2861 (2007).

83. Teixeira, V. Crosstalk between ceramide and cell signalling pathways controlling chronological lifespan in yeast. *PhD thesis, Univ. Porto, Port.* (2015).

84. Jiang, F., Rizavi, H. S. & Greenberg, M. L. Cardiolipin is not essential for the growth of *Saccharomyces cerevisiae* on fermentable or non-fermentable carbon sources. *Mol. Microbiol.* **26,** 481–491 (1997).

85. Patil, V. A., Fox, J. L., Gohil, V. M., Winge, D. R. & Greenberg, M. L. Loss of Cardiolipin Leads to Perturbation of Mitochondrial and Cellular Iron Homeostasis. *J. Biol. Chem.* **288,** 1696–1705 (2013).

86. Lee, Y.-J. *et al.* Sphingolipid signaling mediates iron toxicity. *Cell Metab.* **16,** 90–96 (2012).

87. Kupchak, B. R. *et al.* Probing the Mechanism of *FET3* Repression By Izh2p Overexpression. *Biochim. Biophys. Acta* **1773,** 1124–1132 (2007).

88. Villa, N. Y. *et al.* Sphingolipids function as downstream effectors of a fungal PAQR. *Mol. Pharmacol.* **75,** 866–875 (2009).

89. Kitagaki, H. *et al. ISC1*-dependent metabolic adaptation reveals an indispensable role for mitochondria in induction of nuclear genes during the diauxic shift in *Saccharomyces cerevisiae*. *J. Biol. Chem.* **284,** 10818–10830 (2009).

90. Barbosa, A. D. *et al.* Role for Sit4p-dependent mitochondrial dysfunction in mediating the shortened chronological lifespan and oxidative stress sensitivity of Isc1p-deficient cells. *Mol. Microbiol.* **81,** 515–527 (2011).

91. Teixeira, V., Medeiros, T. C., Vilaça, R., Moradas-ferreira, P. & Costa, V. Reduced TORC1 signaling abolishes mitochondrial dysfunctions and shortened chronological lifespan of Isc1p-deficient cells. *Microb. cell* **1,** 21–36 (2014).

92. Barbosa, A. D. *et al.* Activation of the Hog1p kinase in Isc1p-deficient yeast cells is associated with mitochondrial dysfunction, oxidative stress sensitivity and premature aging. *Mech. Ageing Dev.* **133,** 317–330 (2012).

93. Petrova, V. Y., Drescher, D., Kujumdzieva, A. V. & Schmitt, M. J. Dual targeting of yeast catalase A to peroxisomes and mitochondria. *Biochem. J.* **380,** 393–400 (2004).

94. Betz, C., Zajonc, D., Moll, M. & Schweizer, E. *ISC1*-encoded inositol phosphosphingolipid phospholipase C is involved in Na+/Li+ halotolerance of *Saccharomyces cerevisiae*. *Eur. J. Biochem.* **269,** 4033–4039 (2002).

95. Chang, M., Bellaoui, M., Boone, C. & Brown, G. W. A genome-wide screen for methyl methanesulfonate-sensitive mutants reveals genes required for S phase progression in the presence of DNA damage. *Proc. Natl. Acad. Sci. U. S. A.* **99,** 16934–16939 (2002).

96. Cowart, L. A., Okamoto, Y., Lu, X. & Hannun, Y. A. Distinct roles for de novo versus hydrolytic pathways of sphingolipid biosynthesis in *Saccharomyces cerevisiae*. *Biochem. J.* **393,** 733–740 (2006).

97. Arndt, K. T., Styles, C. A. & Fink, G. R. A suppressor of a *HIS4* transcriptional defect encodes a protein with homology to the catalytic subunit of protein phosphatases. *Cell* **56,** 527–537 (1989).

98. Nickels, J. T. & Broach, J. R. A ceramide-activated protein phosphatase mediates ceramide-induced G1 arrest of *Saccharomyces cerevisiae*. *Genes Dev.* **10,** 382–394 (1996).

99. Sutton, A., Immanuel, D. & Arndt, K. T. The *SIT4* protein phosphatase functions in late G1 for progression into S phase. *Mol. Cell. Biol.* **11,** 2133–2148 (1991).

100. Masuda, C. A., Ramírez, J., Peña, A. & Montero-Lomelí, M. Regulation of monovalent ion homeostasis and pH by the Ser-Thr protein phosphatase *SIT4* in *Saccharomyces cerevisiae*. *J. Biol. Chem.* **275,** 30957–30961 (2000).

101. Zabrocki, P. *et al.* Protein phosphatase 2A on track for nutrient-induced signalling in yeast. *Mol. Microbiol.* **43,** 835–842 (2002).

102. Bhandari, D. *et al.* Sit4p/PP6 regulates ER-to-Golgi traffic by controlling the dephosphorylation of COPII coat subunits. *Mol. Biol. Cell* **24,** 2727–2738 (2013).

103. Angeles de la Torre-Ruiz, M., Torres, J., Arino, J. & Herrero, E. Sit4 Is Required for Proper Modulation of the Biological Functions Mediated by Pkc1 and the Cell Integrity Pathway in *Saccharomyces cerevisiae*. *J. Biol. Chem.* **277,** 33468–33476 (2002).

104. Jablonka, W., Guzmán, S., Ramírez, J. & Montero-Lomelí, M. Deviation of carbohydrate metabolism by the *SIT4* phosphatase in *Saccharomyces cerevisiae*. *Biochim. Biophys. Acta - Gen. Subj.* **1760,** 1281–1291 (2006).

105. Di Como, C. J. & Arndt, K. T. Nutrients, via the Tor proteins, stimulate the association of Tap42 with type 2A phosphatases. *Genes Dev.* **10,** 1904–1916 (1996).

106. Brewster, J. L., de Valoir, T., Dwyer, N. D., Winter, E. & Gustin, M. C. An osmosensing signal transduction pathway in yeast. *Science* **259,** 1760–1763 (1993).

107. Galcheva-Gargova, Z., Derijard, B., Wu, I. H. & Davist, R. J. Osmosensing signal transduction pathway in mammalian cells. *Science (80-.).* **265,** 806–808 (1994).

108. Han, J., Lee, J. D., Bibbs, L. & Ulevitch, R. J. A MAP kinase targeted by endotoxin and hyperosmolarity in mammalian cells. *Science (80-.).* **265,** 808–811 (1994).

109. Willaime-Morawek, S., Brami-Cherrier, K., Mariani, J., Caboche, J. & Brugg, B. C-Jun N-terminal kinases/c-Jun and p38 pathways cooperate in ceramide-induced neuronal apoptosis. *Neuroscience* **119,** 387–397 (2003).

110. Kong, J. Y., Klassen, S. S. & Rabkin, S. W. Ceramide activates a mitochondrial p38 mitogen-activated protein kinase: A potential mechanism for loss of mitochondrial transmembrane potential and apoptosis. *Mol. Cell. Biochem.* **278,** 39–51 (2005).

111. Loewith, R. *et al.* Two *TOR* complexes, only one of which is rapamycin sensitive, have distinct roles in cell growth control. *Mol. Cell* **10,** 457–468 (2002).

112. Loewith, R. & Hall, M. N. Target of rapamycin (*TOR*) in nutrient signaling and growth control. *Genetics* **189,** 1177–1201 (2011).

113. Bonawitz, N. D., Chatenay-Lapointe, M., Pan, Y. & Shadel, G. S. Reduced *TOR* Signaling Extends Chronological Life Span via Increased Respiration and Upregulation of Mitochondrial Gene Expression. *Cell Metab.* **5,** 265–277 (2007).

114. Pan, Y., Schroeder, E. A., Ocampo, A., Barrientos, A. & Shadel, G. S. Regulation of Yeast Chronological Life Span by TORC1 via Adaptive Mitochondrial ROS Signaling. *Cell Metab.* **13,** 668–678 (2011).

115. Swinnen, E., Ghillebert, R., Wilms, T. & Winderickx, J. Molecular mechanisms linking the evolutionary conserved TORC1-Sch9 nutrient signalling branch to lifespan regulation in *Saccharomyces cerevisiae*. *FEMS Yeast Res.* **14,** 17–32 (2014).

116. Murray, A. W. Colony PCR. at <http://www.mcb.harvard.edu/murray/colony_pcr.html>

117. Mason, D. A. *et al.* Increased nuclear envelope permeability and Pep4p-dependent degradation of nucleoporins during hydrogen peroxide-induced cell death. *FEMS Yeast Res.* **5,** 1237–1251 (2005).

118. Gietz, R. D. & Schiestl, R. H. High-efficiency yeast transformation using the LiAc/SS carrier DNA/PEG method. *Nat. Protoc.* **2,** 31–4 (2007).

119. Hanahan, D., Techniques for transformation of *E. coli*. *DNA cloning*. **1**, 109-135 (1985).

120. Tamarit, J., Irazusta, V., Moreno-Cermeño, A. & Ros, J. Colorimetric assay for the quantitation of iron in yeast. *Anal. Biochem.* **351,** 149–51 (2006).

121. Daum, G., Bohni, P. C. & Schatzg, G. Import of Proteins into Mitochondria. Cytochrome b2 and cytochrome c peroxidase are located in the intermembrane space of yeast mitochondria. *J. Biol. Chem.* **257,** 13042–13047 (1982).

122. Vilaça, R. *et al.* Sphingolipid signalling mediates mitochondrial dysfunctions and reduced chronological lifespan in the yeast model of Niemann-Pick type C1. *Mol. Microbiol.* **91,** 438–451 (2014).

123. Leite, A. *et al.* Discrimination of fluorescence light-up effects induced by pH and metal ion chelation on a spirocyclic derivative of rhodamine B. *Dalton Trans.* **42,** 6110–6118 (2013).

124. Schneider, C.A., Rasband, W.S. & Eliceiri, K.W. NIH Image to ImageJ: 25 years of image analysis. *Nature Methods* **9**, 671-675 (2012).

125. Urrutia, P. J., Mena, N. P. & Núñez, M. T. The interplay between iron accumulation, mitochondrial dysfunction, and inflammation during the execution step of neurodegenerative disorders. *Front. Pharmacol.* **5,** 38(1–12) (2014).

126. Seo, A. Y. *et al.* Mitochondrial iron accumulation with age and functional consequences. *Aging Cell* **7,** 706–716 (2008).

127. Valko, M., Morris, H. & Cronin, M. T. Metals, toxicity and oxidative stress. *Curr. Med. Chem.* **12,** 1161–1208 (2005).

128. Matmati, N. & Hannun, Y. A. Thematic review series: sphingolipids. *ISC1* (inositol phosphosphingolipid-phospholipase C), the yeast homologue of neutral sphingomyelinases. *J. Lipid Res.* **49,** 922–928 (2008).

129. Moore, R. E., Kim, Y. & Philpott, C. C. The mechanism of ferrichrome transport through Arn1p and its metabolism in *Saccharomyces cerevisiae*. *Proc. Natl. Acad. Sci. U. S. A.* **100,** 5664–5669 (2003).

130. Lee, K.-T., Lee, J.-W., Lee, D., Jung, W.-H. & Bahn, Y.-S. A Ferroxidase, Cfo1, Regulates Diverse Environmental Stress Responses of *Cryptococcus neoformans* through the HOG Pathway. *Mycobiology* **42,** 152–157 (2014).

131. Kaba, H. E. J., Nimtz, M., Müller, P. P. & Bilitewski, U. Involvement of the mitogen activated protein kinase Hog1p in the response of *Candida albicans* to iron availability. *BMC Microbiol.* **13,** 16(1–15) (2013).